STUDY OF CARBON DIOXIDE SENSING CHARACTERISTICS OF NANOCRYSTALLINE BARIUM TITANATE

Thesis is submitted in partial fulfilment of the requirement for the degree of

MASTER OF TECHNOLOGY IN LASER TECHNOLOGY

By

AVANISH KUMAR

Examination Roll No.: **M4LST23006**

Registration No.: **160421 of 2021-22**

Under the guidance of:

Prof. Siddhartha Bhattacharyya

Faculty of Interdisciplinary Studies, Law and Management, Jadavpur University, Kolkata

Dr. Jiten Ghosh

Pr. Scientist, XRD and SEM Units, Materials Characterization Div. ; Associate Professor, AcSIR, CSIR-Central Glass and Ceramic Research Institute, Kolkata

School of Laser Science and Engineering

Faculty of Interdisciplinary Studies, Law and Management

Jadavpur University

Kolkata -700032

India

June 2023

FACULTY OF INTERDISCIPLINARY STUDIES, LAW AND MANAGEMENT

JADAVPUR UNIVERSITY

KOLKATA -700032

CERTIFICATE OF RECOMMENDATION

We hereby recommend that the thesis presented by Mr. AVANISH KUMAR titled "**STUDY OF CARBON DIOXIDE SENSING CHARACTERISTICS OF NANOCRYSTALLINE BARIUM TITANATE"** was under our supervision and is accepted in partial fulfilment of the degree of Master of Technology in Laser Technology during the academic session 2021- 2023.

(Thesis Advisor)

Date:

Seal:

(Thesis Advisor)

Date:

Seal:

Countersigned by:

(Director)

(School of Laser Science and Engineering)

Date:

Seal:

(Dean)

(Faculty Of Interdisciplinary Studies, Law And Management)

Date:

Seal:

SCHOOL OF LASER SCIENCE AND ENGINEERING

FACULTY OF INTERDISCIPLINARY STUDIES, LAW AND MANAGEMENT

JADAVPUR UNIVERSITY

KOLKATA -700032

DECLARATION OF ORIGINALITY AND

COMPLIANCE OF ACADEMIC ETHICS

I hereby declare that this thesis contains literature survey and original research work by the undersigned candidate, as part of my Master of Technology in Laser Technology studies during the academic session 2021-2023.

All information in this document has been obtained and presented in accordance with academic rules and ethical conduct.

I also declare that, as required by these rules and conduct, I have fully cited and referred to all material and results that are not original to this work.

Name: **AVANISH KUMAR**

Examination Roll Number: **M4LST23006**

Thesis Title: **STUDY OF CARBON DIOXIDE SENSING CHARACTERISTICS OF NANOCRYSTALLINE BARIUM TITANATE.**

Signature:

Dated:

FACULTY OF INTERDISCIPLINARY STUDIES, LAW AND MANAGEMENT

JADAVPUR UNIVERSITY

KOLKATA -700032

CERTIFICATE OF APPROVAL *

This foregoing thesis is hereby approved as a credible study of an engineering subject carried out and presented in a manner satisfactory to warrant its acceptance as a prerequisite to the degree for which it has been submitted. It is understood that by this approval the undersigned do not necessarily endorse or approve any statement made, opinion expressed or conclusion drawn therein but approve the thesis only for the purpose for which it has been submitted.

Committee On Final Examination For Evaluation Of Thesis

Signature:

Date:

Seal:

Signature:

Date:

Seal:

Signature:

Date:

Seal:

* Only in case the the thesis is approved

LIST OF FIGURES

LIST OF TABLES

ACKNOWLEDGEMENTS

First and foremost, I would like to express my sincere gratitude to my supervisors **Dr. Jiten Ghosh** (Pr. Scientist, XRD and SEM Units, Materials Characterization Div.; Associate Professor, AcSIR, CSIR-Central Glass and Ceramic Research Institute, Kolkata) and **Prof. Siddhartha Bhattacharyya** (Faculty of Interdisciplinary Studies, Law and Management, Jadavpur University, Kolkata) for their invaluable guidance, unwavering support, and continuous encouragement throughout the course of my M.Tech thesis. Their expertise, profound knowledge, and insightful feedback have been instrumental in shaping this research work.

Dr. Jiten Ghosh's expertise as a Principal Scientist in XRD and SEM Units, Materials Characterization Division, and his experience as an Associate Professor in AcSIR, CSIR-Central Glass and Ceramic Research Institute, Kolkata, have been instrumental in shaping this research work. Prof. Siddhartha Bhattacharyya, from the Faculty of Interdisciplinary Studies, Law, and Management at Jadavpur University, Kolkata, has provided profound knowledge and insightful feedback, enhancing the quality of the research. His dynamism, fantastic stamina and day-to-day monitoring in every minute detail were a constant source of inspiration to me.

I would also like to express my sincere gratitude to Prof. Dipten Misra, Director, School of Laser Science and Engineering, Jadavpur University, for his constant guidance, tireless support and encouragement. I am also thankful to all the faculty, classmates and seniors of the School of Laser Science and Engineering for vibrant atmosphere, everlasting encouragement, and help in need.

I also express sincere gratitude to Dr. Suman Kumari Mishra, Director, CSIR-CGCRI, Kolkata for providing me with an opportunity for carrying out my M. Tech project at CSIR-CGCRI, Kolkata. I am also thankful to Dr.Tarun Kumar Kayal (chief scientist & head, MCD), for providing opportunity to work in the Material Characterization Division of CSIR-CGCRI.

I would like to thank Dr. Jiten Ghosh again for guiding me to carry out different experiments at MCD division.

I am also thankful to Mr. Nirmal Ghosh, Mr. Prosenjit Khan, Ashok Kr Mandal, Kajari Dasgupta, Moumita Sha, Bhola Nath Jana, Shahnoor Islam, Kanchan Kole, Subrato Pramanik, Sumit Nath, Ashish Jana, Amit Meity and others for support, assistance and guidance during different experiments at CGCRI.

I would like to offer special thanks to Santanu Sen, Chief Scientist, Instrumentation Section, CSIR-CGCRI for constant monitoring, support and encouragement in the research work as well as, for guiding to use impedence spectrometry instruments.

I am indebted to my friends for their camaraderie, stimulating discussions, and support throughout my M.Tech project. Their unwavering belief in my abilities has been a driving force behind my accomplishments.

I am grateful to my family for their unconditional love, encouragement, and sacrifices. Their unwavering support and belief in my aspirations have been the pillars of my success.

Finally, I would like to express my gratitude to all the individuals who have directly or indirectly contributed to the completion of this thesis. Their assistance, whether through discussions, technical support, or providing necessary resources, has been invaluable.

AVANISH KUMAR

ABSTRACT

Barium titanate ceramic is a highly significant ferroelectric material with widespread usage in the electronic industries, particularly in the production of multi-layer ceramic capacitors (MLCC). As electronic devices continue to shrink in size, the influence of size on the dielectric properties of $BaTiO_3$ perovskite has gained remarkable importance. The ongoing trend of miniaturization has sparked interest in exploring the functional properties of this material at the nano-scale.

Among the various methods available, mechanical milling stands out as the simplest and most cost-effective technique for obtaining nanostructured materials from bulk sources. High-energy ball milling has proven effective in producing nanocrystalline $BaTiO_3$ perovskite, inducing structural relaxation in surface atoms and generating inhomogeneous strain through the introduction of defects in crystalline solids. These defects play a crucial role in influencing the properties of the resulting powder. Notably, the presence of defects leads to a reaction between the nanostructured $BaTiO_3$ and atmospheric carbon dioxide, resulting in the formation of $BaCO_3$.

This project focuses on investigating the carbon dioxide sensing characteristics of nanocrystalline $BaTiO_3$, utilizing the effects of CO_2 on the structural and dielectric properties of this material. Several techniques, including X-ray diffraction (XRD), field emission scanning electron microscopy (FESEM), transmission electron microscopy (TEM), energy-dispersive X-ray spectroscopy (EDX), and impedance spectrometry, have been employed to assess changes in the structure and dielectric measurements and establish correlations with the gas sensing characteristics.

The ultimate goal of this study is to explore the practical applications of nanocrystalline $BaTiO_3$ in CO_2 gas sensors. By investigating the distinct properties of nanocrystalline $BaTiO_3$, this research could offer valuable insights to explore its possible applications in various sensing devices, such as laser in-process sensing, laser safety, and optoelectronic devices due to its ferroelectric, piezoelectric, and photorefractive properties.

TABLE OF CONTENTS

Chapter 1
Introduction

Sustainable development is of paramount importance in addressing the challenges posed by climate change, resource depletion, and environmental degradation. It aims to meet the needs of the present generation without compromising the ability of future generations to meet their own needs. Central to sustainable development is the concept of balancing economic growth, social well-being, and environmental protection[1].

Carbon dioxide (CO_2) levels play a crucial role in sustainable development due to their direct correlation with climate change. CO_2 is a greenhouse gas that traps heat in the Earth's atmosphere, leading to the greenhouse effect and subsequent global warming. The excessive accumulation of CO_2 in the atmosphere, primarily from human activities such as burning fossil fuels and deforestation, has contributed to the intensification of climate change and adverse impact on the environment[2]. In recent years, the issue of rising carbon dioxide levels and its impact on the environment has garnered significant attention worldwide. As a potent greenhouse gas, CO_2 emissions are major contributors to global warming and climate change.

Monitoring and controlling CO_2 levels are essential for sustainable development. High CO_2 concentrations can have detrimental effects on both human health and the environment. Elevated CO_2 levels in indoor spaces, for example, can lead to poor air quality, which can cause respiratory problems, reduced cognitive function, and discomfort. Furthermore, excessive CO_2 emissions contribute to climate change, leading to rising temperatures, sea-level rise, extreme weather events, and the disruption of ecosystems[3-6].

Developing efficient and reliable gas sensing technologies to monitor and control CO_2 levels has become crucial in various sectors, including industrial processes, automotive systems, and environmental monitoring. Monitoring and mitigating CO_2 emissions have become critical for sustainable development and ensuring the well-being of future generations. The global increase in carbon dioxide emissions and its detrimental impact on the environment and human health have fueled the urgency to develop efficient sensing technologies for monitoring CO_2 levels. CO_2 sensing technology plays a crucial role in sustainable development by enabling the accurate and real-time monitoring of CO_2 levels. CO_2 sensors are designed to detect and measure the concentration of CO_2 in various environments, including indoor spaces, industrial settings, and outdoor air. By providing continuous data on CO_2 levels, these sensors facilitate informed decision-making and the implementation of effective mitigation strategies[7-9].

In the context of sustainable buildings, CO_2 sensing is vital for ensuring healthy indoor air quality and optimizing energy efficiency. High CO_2 concentrations are often indicative of inadequate ventilation, which can lead to discomfort, reduced productivity, and health issues. CO_2 sensors help identify these conditions, prompting timely interventions such as increased ventilation or air purification measures. Moreover, optimizing ventilation based on CO_2 levels can significantly reduce energy consumption and associated greenhouse gas emissions, contributing to sustainable energy management[10-11].

CO_2 sensing also plays a pivotal role in environmental monitoring and climate change mitigation. By accurately measuring CO_2 emissions from industrial processes, transportation, and other sources, CO_2 sensors assist in identifying significant contributors to greenhouse gas emissions. This data enables policymakers, businesses, and communities to develop and implement effective strategies to reduce emissions, transition to cleaner energy sources, and promote sustainable practices[12-14].
Therefore, sustainable development necessitates effective management of CO_2 levels, as they are a critical driver of climate change and environmental degradation. CO_2

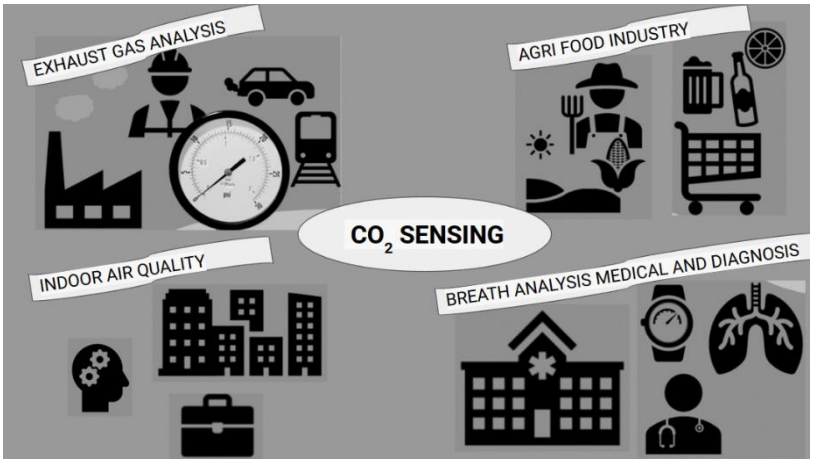

Figure 1.1 Applications of CO_2 sensing; modified from [26].

sensing technology plays a vital role in sustainable development by providing real-time data on CO_2 concentrations, enabling informed decision-making, optimizing energy efficiency, improving indoor air quality, and facilitating effective mitigation strategies. By integrating CO_2 sensing into sustainable practices, we can move towards a more sustainable future that balances economic growth, social well-being, and environmental protection.

Carbon dioxide sensors play a crucial role in various applications, such as indoor air quality control, industrial processes, and environmental monitoring. In this context, nanomaterials have emerged as promising candidates due to their unique properties and enhanced performance compared to their bulk counterparts. Nanocrystalline materials have garnered significant attention in recent years for their unique properties and potential applications. Among these materials, nanocrystalline barium titanate ($BaTiO_3$) has emerged as a promising candidate for gas sensing applications due to its high surface area, enhanced electrical properties, and excellent chemical stability. Harnessing the potential of nanocrystalline $BaTiO_3$ in CO_2 sensing can contribute to the development of innovative sensing technologies[15-18].

1.1. Significance of Nanostructured Barium Titanate Perovskite material

In the realm of advanced materials, perovskites have emerged as a fascinating class of compounds with remarkable properties and diverse applications. One such compound that has garnered significant attention is barium titanate ($BaTiO_3$). Barium titanate belongs to the perovskite family, which is characterized by its distinctive crystal structure and unique electrical and optical properties.

The structural family of perovskites is a large family of compounds having crystal structures related to the mineral perovskite $CaTiO_3$. In the ideal form the crystal structure of cubic ABX_3 perovskite can be described as consisting of corner sharing $[BX_6]$ octahedra with the A cation occupying the 12-fold coordination site formed in the middle of the cube of eight such octahedra (Figure 1.2a). The ideal cubic perovskite structure is not very common and also the mineral perovskite itself is slightly distorted.

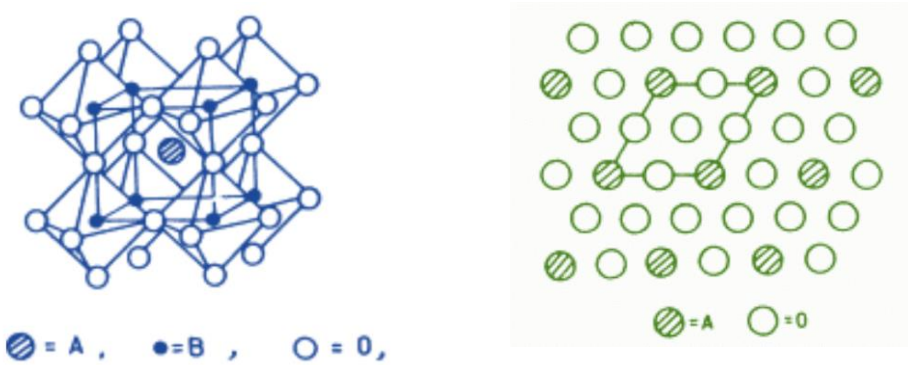

***Figure 1.2 (a)The ABO_3 perovskite structure. (b) Close-packed AO_3 layer in perovskites; modified from* [19].**

Pioneering structural work on perovskites we re conducted by Goldschmidt et al[27] in the 1920's that formed the basis for further exploration of the perovskite family of compounds. Distorted perovskites have reduced symmetry, which is important for their magnetic and electric properties[19-22].

In the ideal cubic case, the cell axis, a, is geometrically related to the ionic radii (r_A, r_B, and r_X) as described in equation:

$$a = \sqrt{2}\,(r_A + r_X) = 2\,(r_B + r_X)$$

Goldschmidt found that the perovskite structure is retained in ABX3 compounds even when this relation is not exactly obeyed and defined a tolerance factor, *t*, as

$$t = \frac{r_A + r_X}{\sqrt{2}(r_B + r_X)}$$

For the ideal perovskite structure, t = 1. The perovskite structure is, however, found for lower values of t ($\sim 0.75 < t \leq 1.0$), also. In such cases, the structure distorts to tetragonal, rhombohedral, or orthorhombic symmetry. This distortion arises from the smaller size of the A ion, which causes a tilting of the BX6 octahedra in order to optimize A–X bonding. Perovskite oxides, ABO_3, can be thought of as consisting of alternating BO_2 and AO layers stacked one over the other in the [001] direction.

An alternative description of the ABO_3 structure in terms of close packing of A and O ions is one where close-packed AO_3 layers (Figure 3.1b) are stacked one over the other with the B cations occupying octahedral holes surrounded by oxygen.

Barium Titanate is a ferroelectric ceramic material that has a rich history in the field of material sciences. Its discovery dates back to the early 1940s when researchers first synthesized and characterized its unique properties.

The history of Barium Titanate begins with the search for new dielectric materials during World War II. **Dielectrics** are materials that can store electrical energy in the form of an electric field. Researchers were looking for materials that could improve the performance of **capacitors**, which are essential components in electronic devices. Barium titanate ($BaTiO_3$, BT) ceramics were discovered during World War II independently in three countries: the US, by Wainer and Salomon [23] in 1942, Japan by Ogawa [24] in 1944, and Russia by Vul [25] in 1944. Barium Titanate exhibited a high dielectric constant and excellent ferroelectric properties, making it a promising candidate for capacitor applications.

The significance of Barium Titanate lies in its **ferroelectricity**, which refers to its ability to switch and retain a permanent electric polarization when an electric field is applied. Ferroelectric materials are known for their ability to exhibit spontaneous electric polarization that can be reversed by an external electric field. Barium titanate is one such ferroelectric material that exhibits a **high Curie temperature**, meaning it retains its ferroelectric properties even at elevated temperatures. The ferroelectric behavior of barium titanate makes it highly desirable for a wide range of applications. In the field of electronics, it is used as a key component in the production of capacitors, where its **high dielectric constant** and **low loss factor** are advantageous. These properties allow for the storage and release of electric charge in a compact and efficient manner. Barium Titanate-based capacitors have been widely used in electronic devices, telecommunications, and power distribution systems.

Furthermore, barium titanate has **piezoelectric properties**, which means it can generate an electric charge when subjected to mechanical stress and, conversely, undergo mechanical deformation when an electric field is applied. This property has led to its use in **transducers, sensors, actuators, and acoustic devices**. The ability to control and manipulate the properties of Barium Titanate, such as its grain size and doping, has further expanded its applications in areas such as **catalysis, energy storage, biomedical devices and sensing applications**.[2]

In addition to its electrical properties, **barium titanate is also known for its optical characteristics**. It exhibits **photorefractive properties**, enabling it to change its refractive index under the influence of light. This property has been harnessed for applications such as **holography and optical data storage.**

Overall, the significance of barium titanate in material sciences lies in its multifaceted properties and its potential for various technological applications. **Its ferroelectric, piezoelectric, and optical properties make it a valuable material in the**

development of electronic devices, sensors, actuators, and energy storage systems. In recent years, exploration of its properties at the nanoscale has led to the development of **nanocrystalline Barium Titanate, which exhibits enhanced properties and offers new possibilities in various applications**. Nanocrystalline forms of barium titanate exhibit unique properties such as enhanced surface area, improved electrical characteristics, and increased sensitivity. Researchers are actively studying and modifying its characteristics to optimize its performance and explore novel applications. Ongoing research continues to explore and harness the potential of barium titanate, contributing to advancements in various fields and driving innovation in material sciences.

Nanocrystalline barium titanate ($BaTiO_3$) offers several advantages over its bulk counterpart, making it a promising material for various research applications. Here are the advantages of nanocrystalline barium titanate:

- **Enhanced Surface Area**: Nanocrystalline barium titanate possesses a high surface-to-volume ratio due to the smaller grain size and increased number of grain boundaries. This results in a larger surface area, allowing for improved interactions with the surrounding environment and enhanced sensitivity in sensing applications.
- **Improved Electrical Properties**: The nanoscale structure of barium titanate leads to improved electrical properties such as increased dielectric constant, enhanced ferroelectric behavior, and reduced electrical leakage. These enhanced electrical characteristics make it suitable for applications in capacitors, energy storage devices, and sensors.
- **Size-Dependent Properties**: The properties of nanocrystalline materials often exhibit size-dependent behavior. As the particle size decreases, quantum effects and surface phenomena become more prominent, leading to unique electrical, optical, and catalytic properties. This size-dependent behavior of nanocrystalline barium titanate enables tailoring its properties for specific research applications.
- **Tunable Properties**: By controlling the synthesis parameters and doping techniques, the properties of nanocrystalline barium titanate can be tailored to specific requirements. This tunability allows researchers to customize the material's characteristics, such as its bandgap, dielectric response, and ferroelectric behavior, to suit different research applications.
- **Versatile Applications**: Nanocrystalline barium titanate finds applications in various research fields, including **electronics, energy storage, catalysis, sensors**, **and biomedical devices**. Its unique properties and versatile nature make it an attractive material for exploring novel research avenues**.**

Thus, nanocrystalline barium titanate offers advantages such as enhanced surface area, improved electrical properties, size-dependent behavior, chemical stability, tunability, and versatile applications. These advantages make it a promising material for diverse research applications, paving the way for innovative advancements in various scientific disciplines.

Nanocrystalline barium titanate (nano-BT) exhibits a wide range of applications across various fields due to its unique properties and versatile nature. The following are some notable applications of nano-BT:

- Electronics: Nanocrystalline barium titanate is widely used in electronics for its ferroelectric properties. It is employed in **capacitors, varistors, and memory devices.** The high dielectric constant and low dielectric loss of nanocrystalline barium titanate make it ideal for **energy storage and signal processing** applications.

- Sensors: Nanocrystalline barium titanate-based sensors are used in diverse fields. Gas sensors utilize its high surface area to detect and measure gases like carbon monoxide (CO) and nitrogen dioxide (NO_2). Pressure sensors benefit from its piezoelectric properties, converting mechanical stress into electrical signals. Additionally, nanocrystalline barium titanate-based humidity sensors find applications in environmental monitoring and industrial processes.

- Energy Harvesting: The piezoelectric properties of nanocrystalline barium titanate make it suitable for energy harvesting applications. It can convert mechanical vibrations or strain into electrical energy, which can be utilized in self-powered sensors, wearable devices, and wireless sensor networks.

- Actuators: Nanocrystalline barium titanate-based actuators find use in precision **positioning systems, robotics, and microelectromechanical systems** (MEMS). These actuators convert electrical energy into mechanical motion, enabling precise control and movement in various applications.

- Biomedical Applications: Nanocrystalline barium titanate has shown promise in biomedical applications such as drug delivery systems, bioimaging, and tissue engineering. Its biocompatibility, tunable properties, and ability to interact with biological systems make it suitable for targeted drug delivery and imaging techniques.

- **Optoelectronics:** Nanocrystalline barium titanate is used in optoelectronic devices such as light-emitting diodes (**LEDs)** and **photodetectors**. Its unique optical properties, including photoluminescence and nonlinear optical effects, make it valuable for applications in **optical communications, displays, and sensors**.

These are just a few examples of the wide-ranging applications of nanocrystalline barium titanate. The versatility and exceptional properties of this material make it a promising candidate for continued research and development across various fields, driving innovations and advancements in technology.

1.2 Overview of carbon dioxide sensing

Carbon dioxide sensing holds significant importance due to its crucial role in various areas, including environmental monitoring, industrial processes, and human health. Understanding and monitoring CO_2 levels is vital for several reasons.

Firstly, CO_2 is a major greenhouse gas directly linked to climate change. Monitoring CO_2 concentrations helps in assessing and understanding the impact of human activities on the Earth's atmosphere. By measuring and analyzing CO_2 levels, scientists and policymakers can gain insights into the effectiveness of climate change mitigation strategies and the progress towards reducing greenhouse gas emissions.

Secondly, CO_2 sensing is vital for maintaining indoor air quality. Elevated CO_2 levels in enclosed spaces, such as homes, offices, and schools, can indicate poor ventilation and the accumulation of other pollutants. Monitoring CO_2 levels helps ensure a healthy indoor environment, as excessive CO_2 concentrations can lead to discomfort, reduced cognitive function, and health issues. By detecting and addressing high CO_2 levels, appropriate ventilation and air quality control measures can be implemented to create safer and more productive indoor environments.

Furthermore, CO_2 sensing plays a crucial role in industrial processes. In manufacturing, energy production, and other industrial sectors, monitoring CO_2 emissions is essential for reducing the carbon footprint and improving energy efficiency. Accurate CO_2 measurements enable businesses to optimize their processes, identify areas for improvement, and implement strategies to reduce greenhouse gas emissions.
Moreover, CO_2 sensing is crucial for the development and deployment of carbon capture and storage (CCS) technologies. CCS aims to capture CO_2 emissions from power plants and industrial facilities, preventing them from entering the atmosphere. Accurate CO_2 sensing is necessary to monitor and verify the effectiveness of CCS systems in reducing greenhouse gas emissions.

Additionally, CO_2 sensing has applications in areas such as agriculture and healthcare. In agriculture, monitoring CO_2 levels in greenhouses helps optimize plant growth and productivity. In healthcare settings, monitoring exhaled CO_2 levels can provide valuable information about respiratory function and assist in diagnosing and managing respiratory disorder.

Carbon dioxide sensing techniques encompass a range of methods and technologies used to detect and quantify CO_2 concentrations in different environments. These techniques are crucial for environmental monitoring, indoor air quality control, climate change research, and various industrial applications. Here is an overview of some common carbon dioxide sensing techniques:

Non-dispersive infrared (NDIR) sensing: NDIR sensors use the principle of infrared absorption to measure CO_2 concentrations. They emit infrared light at specific wavelengths that are absorbed by CO_2 molecules. The amount of absorbed light is proportional to the CO_2 concentration, allowing for accurate measurements.

Chemical gas sensors: These sensors utilize chemical reactions between CO_2 and specific chemicals to detect its presence. For example, CO_2 can react with certain metal oxides or organic compounds, causing a change in electrical conductivity or optical properties that can be measured.

Solid-state sensors: Solid-state sensors employ materials such as metal oxides, polymers, or nanomaterials that undergo changes in electrical properties when exposed to CO_2. These changes can be measured and correlated with CO_2 concentrations.
Electrochemical sensors: Electrochemical sensors utilize an electrochemical cell to measure CO_2 concentrations. The cell contains electrodes that undergo chemical reactions with CO_2, producing an electrical signal that is proportional to the CO_2 concentration.

Photoacoustic spectroscopy: This technique involves using a laser beam to excite CO_2 molecules, resulting in the generation of sound waves. The amplitude of the sound waves is proportional to the CO2 concentration and can be detected and measured.
Optical fiber sensors: Optical fiber-based sensing techniques utilize the interaction between CO2 and light propagating through optical fibers. Changes in light intensity, phase, or wavelength due to CO2 absorption can be detected and quantified.

These are just a few examples of the carbon dioxide sensing techniques available. Each technique has its advantages and limitations, and the choice of method depends on the specific application requirements, accuracy needs, and environmental conditions. Continuous advancements in sensor technology continue to enhance the sensitivity, selectivity, and reliability of carbon dioxide sensing techniques.

1.3 Motivation and Objective for CO_2 sensing using nano-Barium Titanate

The motivation for utilizing nanocrystalline barium titanate ($BaTiO_3$) in carbon dioxide (CO_2) sensing arises from its unique properties and the need for efficient and sensitive CO_2 sensing technologies. Several factors contribute to the motivation for exploring the potential of nanocrystalline $BaTiO_3$ in CO_2 sensing applications.

Firstly, nanocrystalline materials, including nanocrystalline $BaTiO_3$, exhibit enhanced surface area and unique electrical properties compared to their bulk counterparts. The increased surface area allows for greater interaction with the surrounding environment, enabling improved sensing capabilities. The unique electrical properties, such as high dielectric constant and piezoelectricity, make nanocrystalline $BaTiO_3$ a promising material for developing highly sensitive and responsive CO_2 sensors to be used for ppm level sensing.

Moreover, nanocrystalline $BaTiO_3$ offers the advantage of chemical stability, which is crucial for long-term and reliable sensing performance. Its resistance to environmental factors and robustness against harsh conditions make it suitable for various applications where CO_2 sensing is required.

Additionally, the nanocrystalline form of $BaTiO_3$ can be synthesized using scalable and cost-effective methods, making it a viable option for large-scale production of CO_2 sensors. This scalability is crucial for commercialization and widespread adoption of CO_2 sensing technologies.

Furthermore, the integration of nanocrystalline $BaTiO_3$ with other advanced materials and technologies, such as nanoelectronics and microfabrication techniques, opens up possibilities for the development of miniaturized, low-power, and high-performance CO_2 sensing devices.

The objective of the study on CO_2 sensing characteristics using nanocrystalline barium titanate ($BaTiO_3$) is to gain a comprehensive understanding of the sensing performance and capabilities of this material for carbon dioxide detection. The specific objectives can be outlined as follows:

Characterization of Sensing Parameters: The study aims to investigate various sensing parameters such as sensitivity, selectivity, response time, and stability of nanocrystalline $BaTiO_3$-based CO_2 sensors. By systematically analyzing these parameters, researchers can determine the optimal operating conditions and sensor configurations for efficient and accurate CO_2 sensing.

Performance Optimization: The objective is to explore methods to enhance the sensing performance of nanocrystalline $BaTiO_3$ sensors. This may involve optimizing the synthesis and fabrication techniques, exploring different doping or functionalization approaches, or modifying the sensor architecture to improve sensitivity, selectivity, and response time.

Calibration and Validation: The study intends to establish calibration procedures and validate the accuracy and reliability of the nanocrystalline $BaTiO_3$ sensors for CO_2 sensing. This involves comparing the sensor response with reference standards or established measurement techniques to ensure the validity of the obtained CO_2 concentration data.

Environmental Monitoring Applications: The objective is to assess the suitability of nanocrystalline $BaTiO_3$-based CO_2 sensors for environmental monitoring applications. This includes evaluating their performance in different environmental conditions and real-world scenarios, such as indoor air quality monitoring, industrial emissions monitoring, or greenhouse gas monitoring.

Integration and Miniaturization: The study aims to explore the integration of nanocrystalline $BaTiO_3$ CO_2 sensors into miniaturized and portable devices. This objective involves developing sensor arrays, signal processing algorithms, and data communication protocols to enable practical and real-time CO_2 monitoring in various settings.

Chapter 2
Literature Review

In this chapter, we delve into the realm of nanomaterials, particularly Barium Titanate nanoparticles, exploring their synthesis methods, properties at the nano scale, and various applications. Nanomaterials play a crucial role in the field of materials science, offering unique properties and enabling innovative technological advancements.

The section on synthesis methods provides an overview of the different techniques employed to fabricate nanomaterials, including physical, chemical, and biological approaches. Understanding these methods is essential for tailoring the properties and characteristics of nanomaterials to suit specific applications.

Next, we delve into the properties exhibited by materials at the nano scale. Nanomaterials often exhibit distinct physical, chemical, and mechanical properties due to their small size and high surface-to-volume ratio. We explore phenomena such as quantum confinement, surface plasmon resonance, and size-dependent optical, electrical, and magnetic properties. This understanding of nanomaterial properties lays the foundation for leveraging their unique features in various applications.

The chapter further explores the wide range of applications of nanostructured materials. Nanomaterials find application in diverse fields, including electronics, energy storage, catalysis, biomedical devices, environmental remediation, and sensors. We discuss the specific advantages offered by nanomaterials in these applications and highlight their potential to revolutionize industries and address key challenges.

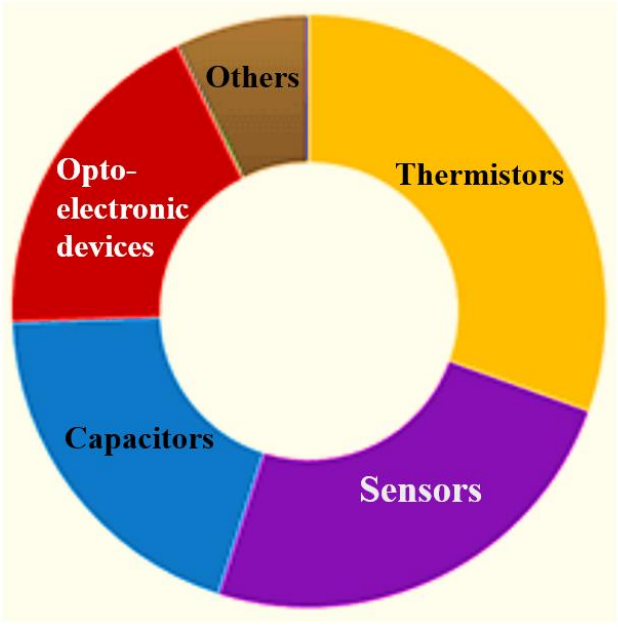

Figure 2.1 Barium Titanate Global Market share by application(%), 2022; modified from [28].

2.1 Synthesis Methods of Barium Titanate nanoparticles

The synthesis of nanomaterials is a critical aspect of nanoscience and nanotechnology, enabling the creation of materials with unique properties and functionalities at the nanoscale. Various synthesis methods are employed in the fabrication of nanomaterials.

These methods can be broadly classified into top-down and bottom-up approaches, each offering distinct advantages and limitations [29].

Bottom-Up Synthesis:

a. Chemical Vapor Deposition (CVD): In CVD, precursor gases are introduced into a chamber, where they undergo chemical reactions to form nanomaterials on a substrate.

b. Sol-Gel Synthesis: This method involves the formation of nanomaterials through the hydrolysis and condensation of precursor molecules in a solution.

c. Hydrothermal Synthesis: Nanomaterials are synthesized by placing reactants in a high-pressure, high-temperature aqueous environment, allowing for controlled nucleation and growth.

d. Electrochemical Deposition: Nanomaterials are electrodeposited onto a substrate by applying an electric current through an electrolyte solution.

Top-Down Synthesis:

a. Ball Milling: Mechanical energy is used to reduce bulk materials into nanoscale particles through repetitive grinding and collision processes.

b. Lithography: Techniques such as electron beam lithography or photolithography are employed to pattern and shape materials at the nanoscale.

c. Laser Ablation: A high-energy laser is focused on a target material, causing vaporization and subsequent condensation into nanoscale particles.

d. Mechanical Attrition: Mechanical forces, such as high-energy milling or grinding, are applied to break down bulk materials into nanoparticles.

Self-Assembly:

a. Templated Growth: A template with predefined nanoscale patterns or pores is used to guide the growth of nanomaterials.

b. Molecular Self-Assembly: Nanomaterials are formed through the spontaneous assembly of molecular components driven by non-covalent interactions.

Biological Methods:

a. Biofabrication: Biological organisms or their components are used to synthesize nanomaterials with controlled structures and properties.

b. Genetic Engineering: Genetic modification techniques are employed to produce nanomaterials through the manipulation of biological systems.

Hybrid Methods:

Hybrid methods combine multiple techniques, such as combining top-down and bottom-up approaches, to achieve desired nanomaterial structures and properties.

It is important to note that the choice of method depends on factors such as the desired nanomaterial properties, scalability, control over size and shape, and the specific application requirements.

There are multiple synthesis methods available for producing $BaTiO_3$ nanoparticles (Figure 2.2). Traditionally, $BaTiO_3$ nanoparticles were prepared through the solid-state reaction between $BaCO_3$ and TiO_2 at elevated temperatures[32]. This method involves high temperatures above 1000 °C and is cost-effective for mass production but not suitable for obtaining nanoparticles. At such high temperatures, atom diffusion occurs,

resulting in grain growth and a reduction in the powder's surface energy. Solid-state reaction also leads to impurities and a wide distribution of grain sizes in the powders. However, in the aftermath of the oil shocks in 1973, alternative techniques were developed to address the energy costs and limitations associated with solid-state reaction[30]. These methods include soft-chemistry approaches, high-energy ball-milling, sol-gel methods, co-precipitation, hydrothermal and solvothermal synthesis, and high-energy milling.

The choice of synthesis method and its parameters significantly influence the size and morphology of the $BaTiO_3$ NPs[34]. Controlling these factors is crucial in achieving desired properties for the NPs. Different synthesis methods offer distinct advantages and limitations. For example, bottom-up synthesis methods allow precise control over the composition and structure of nanomaterials. Chemical Vapor Deposition (CVD) enables the growth of high-quality thin films with excellent control over thickness and uniformity. Sol-Gel Synthesis is suitable for fabricating nanomaterials with complex compositions and morphologies. Hydrothermal Synthesis provides a means to synthesize nanomaterials under specific temperature and pressure conditions, facilitating controlled nucleation and growth.

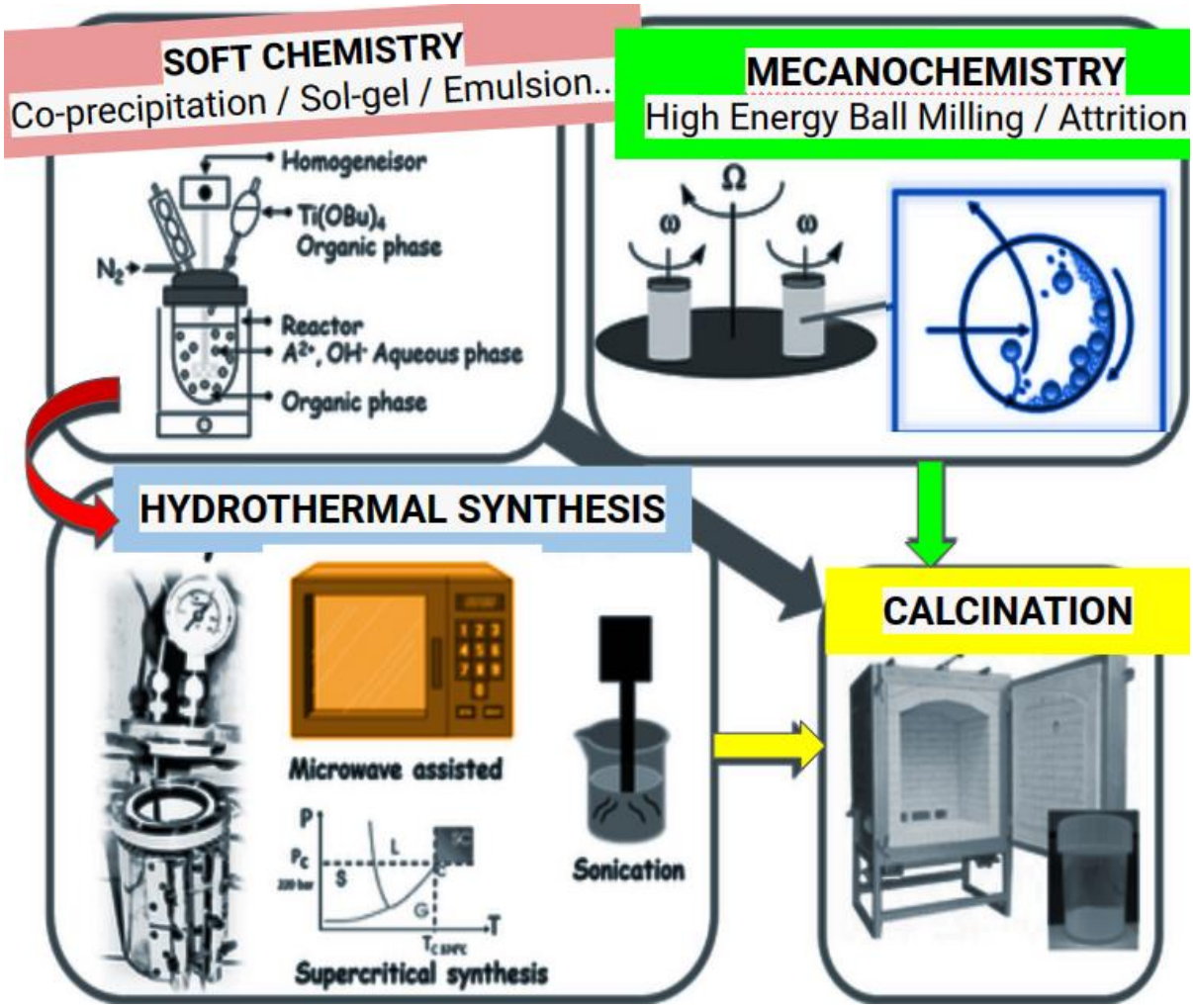

***Figure 2.2 Schematic representation of different synthesis routes for the production of $BaTiO_3$ NPs; modified from* [30].**

On the other hand, top-down synthesis methods are useful for reducing bulk materials to the nanoscale. Ball Milling enables the production of nanoscale particles through mechanical grinding and collision processes. Lithography techniques offer precise patterning and shaping of materials at the nanoscale. Laser Ablation allows the production of nanoparticles through the vaporization and subsequent condensation of target materials. Mechanical Attrition breaks down bulk materials into nanoparticles through mechanical forces.

Additionally, self-assembly methods leverage natural forces or designed templates to guide the formation of nanomaterials. Templated Growth uses predefined patterns or pores to direct the growth of nanomaterials. Molecular Self-Assembly relies on non-covalent interactions to spontaneously assemble molecular components into nanomaterials.

Biological methods utilize biological organisms or genetic engineering techniques to synthesize nanomaterials. Biofabrication exploits biological systems to produce nanomaterials with controlled structures and properties. Genetic Engineering modifies biological systems to enable the production of specific nanomaterials.

Furthermore, hybrid methods combine multiple synthesis techniques to achieve desired nanomaterial structures and properties. By selecting the most appropriate synthesis method, researchers can tailor nanomaterials for specific applications, considering factors such as functionality, scalability, and performance requirements.

2.2 Properties at the Nano Scale

Nanomaterials exhibit a wide range of fascinating properties at the nanoscale, offering unique advantages and possibilities for various applications. Understanding these properties is essential for harnessing the full potential of nanomaterials. Let's delve deeper into the key properties acquired by nanomaterials:

Size-Dependent Properties: At the nanoscale, nanomaterials experience quantum confinement effects, where their properties become size-dependent. This means that as the size of the material decreases, its characteristics can change significantly. For example, the optical absorption, emission, and bandgap energy can be tuned by altering the size of the nanomaterial, enabling tailored optical and electronic properties.

Enhanced Surface Area: One of the most striking features of nanomaterials is their exceptionally high surface area compared to their volume. This enlarged surface area offers numerous benefits. Firstly, it leads to improved reactivity, as a larger surface allows for more interactions with other molecules. Secondly, nanomaterials exhibit enhanced adsorption capacities, making them suitable for applications such as pollutant removal or drug delivery. Lastly, the increased surface area facilitates better interactions with the surrounding environment, enabling sensitive sensors and responsive systems.
Mechanical Properties: Nanomaterials often exhibit remarkable mechanical properties due to their unique structure at the nanoscale. The presence of grain boundaries, defects, and interfaces in nanomaterials can enhance their mechanical characteristics, including

high strength, hardness, and flexibility. These properties make nanomaterials desirable for applications requiring materials with exceptional mechanical performance, such as aerospace components or lightweight structural materials.

Optical and Electronic Properties: Nanoscale materials display intriguing optical and electronic properties. Quantum confinement effects, arising from the confinement of electrons or photons within the nanomaterials, result in size-dependent phenomena. For instance, nanomaterials can emit light of different colors depending on their size, making them useful in optoelectronic devices. Additionally, nanomaterials can exhibit plasmonic effects, which involve the collective oscillation of electrons, enabling enhanced light-matter interactions and novel optical functionalities.

Thermal Properties: The thermal properties of nanomaterials can differ from those of bulk materials. At the nanoscale, phonon scattering becomes more significant, leading to altered thermal conductivity. Nanomaterials with low thermal conductivity find applications in thermal barrier coatings, thermoelectric devices, and heat management systems. Understanding and controlling thermal properties at the nanoscale are crucial for optimizing energy efficiency and thermal stability in various applications.

Chemical Reactivity: Nanomaterials possess high chemical reactivity owing to their increased surface area and unique surface properties. These properties allow nanomaterials to exhibit enhanced catalytic activity, accelerating chemical reactions. Catalytic nanomaterials find applications in various fields, such as pollution control, energy conversion, and industrial processes. By exploiting the tailored surface properties of nanomaterials, researchers can design efficient catalysts for specific chemical transformations.

Magnetic Properties: Nanomaterials can exhibit intriguing magnetic behavior at the nanoscale. The size, composition, and structure of nanomaterials influence their magnetic properties. For example, nanomaterials can display enhanced magnetism, superparamagnetism (temporary magnetism), or magnetic anisotropy (directional magnetism). These magnetic properties make nanomaterials valuable for applications in magnetic storage devices, sensors, and biomedical systems, such as targeted drug delivery or magnetic resonance imaging (MRI).

The exploration and understanding of these properties provide researchers and engineers with the knowledge necessary to design and develop nanomaterials with tailored characteristics for specific applications. By manipulating and optimizing these properties, nanomaterials open up new avenues for technological advancements in electronics, energy storage and conversion, medicine, environmental remediation, and many other fields.

2.3 Applications of nanostructured materials

Nanostructured materials, with their remarkable properties at the nanoscale, have revolutionized numerous fields and enabled significant technological advancements. In this section, we will delve into the diverse applications of nanostructured materials, highlighting their impact in various domains.

Electronics and Optoelectronics: Nanostructured materials have transformed the electronics industry by enabling the development of smaller, faster, and more efficient electronic devices. They are utilized in the fabrication of nanoscale transistors, memory devices, and sensors. The unique properties of nanomaterials, such as high electron mobility and tunable bandgaps, make them ideal for creating nanoelectronic components. Additionally, nanostructured materials find applications in optoelectronic devices like LEDs, solar cells, and photodetectors, benefiting from their enhanced optical and electronic properties.

Biomedical Applications: Nanostructured materials have made significant contributions to biomedical sciences and healthcare. They are utilized in drug delivery systems, imaging agents, tissue engineering scaffolds, and biosensors. The small size and tailored surface properties of nanomaterials enable targeted drug delivery, prolonged drug release, and improved bioavailability. They also enhance imaging contrast in techniques such as magnetic resonance imaging (MRI) and enable precise monitoring of biomarkers. Moreover, nanostructured materials provide the structural framework for tissue engineering, facilitating cell adhesion, proliferation, and differentiation.

Energy Storage and Conversion: Nanostructured materials play a crucial role in advancing energy storage and conversion technologies. They are employed in lithium-ion batteries, supercapacitors, and fuel cells to enhance energy storage capacity, charge/discharge rates, and overall performance. The high surface area and improved electrochemical properties of nanomaterials enable faster ion diffusion and increased energy density. Furthermore, nanostructured materials find applications in solar cells, where they enhance light absorption and charge separation, leading to improved photovoltaic efficiency. They are also utilized as catalysts in energy conversion systems such as water splitting for hydrogen production.

Environmental Remediation: Nanostructured materials offer great potential for addressing environmental challenges. They are used for the removal of pollutants from air and water, such as heavy metals, organic contaminants, and industrial waste. Nanomaterial-based adsorbents, membranes, and photocatalysts exhibit high efficiency in pollutant adsorption, filtration, and degradation. The large surface area and tailored surface chemistry of nanostructures enable effective pollutant capture and conversion, contributing to the development of sustainable environmental remediation technologies.

Coatings and Surface Modification: Nanostructured materials play a vital role in enhancing the performance and durability of various materials through advanced coatings and surface modifications. They provide functionalities such as corrosion resistance, self-cleaning properties, anti-fouling capabilities, and improved mechanical

properties. Nanostructured coatings can protect surfaces from environmental degradation, prevent microbial growth, and reduce friction. These coatings find applications in industries ranging from automotive and aerospace to healthcare and electronics, improving the lifespan and functionality of diverse materials.

These applications represent only a fraction of the wide-ranging potential of nanostructured materials. Their unique properties and versatility continue to inspire innovation across fields, driving advancements in technology, medicine, energy, and environmental sciences. The exploration of these applications in the study of carbon dioxide sensing using nanocrystalline barium titanate expands our understanding of these materials and contributes to their further utilization in practical and sustainable solutions.

Chapter 3
Experimental Details

In this chapter, we delve into the experimental details involved in the investigation of CO_2 sensing characteristics of $BaTiO_3$ nanoparticles. The successful implementation of CO_2 sensors requires a comprehensive understanding of the material synthesis, characterization techniques, and measurement setups. This chapter outlines the methodologies employed to fabricate the $BaTiO_3$ nanoparticles, the characterization techniques utilized to analyze their structural and morphological properties, and the experimental setup for CO_2 sensing measurements.

The synthesis of $BaTiO_3$ nanoparticles plays a crucial role in determining their structural, morphological, and surface properties, which significantly influence their sensing performance. In section 3.1, we present the specific methods used for the formation of $BaTiO_3$ nanoparticles. We discuss the selection of precursors, reaction conditions, and the synthesis technique utilized, highlighting the advantages and limitations of the chosen approach.

Accurate characterization of the synthesized nanoparticles is essential to understand their crystal structure, particle size, composition and other relevant properties. In section 3.2, we discuss the characterization techniques employed to investigate the structural and morphological features of the nanoparticles, the principles and instrumentation of various characterization techniques, including scanning electron microscopy (SEM), transmission electron microscopy (TEM) and X-ray diffraction (XRD). We explain how each technique provides valuable insights into the properties of the nanoparticles, enabling us to assess their suitability for CO_2 sensing applications.

Additionally, we outline the procedures followed for sample preparation, such as the preparation of pellets, ultrasonication, thin films or deposition onto substrates, which are necessary for subsequent sensing experiments. The selection of appropriate deposition techniques and substrates is also discussed in this section.

After synthesizing and characterizing the $BaTiO_3$ nanoparticles, we performed CO_2 sensing measurements to evaluate their sensing characteristics. In this section, we describe the experimental setup used for CO_2 sensing measurements, including the gas chamber, temperature and humidity control systems, and the measurement apparatus. We explain the protocol followed to measure the response and recovery characteristics of the $BaTiO_3$ nanoparticles in the presence of varying CO_2 concentrations. Furthermore, we discuss the data acquisition and analysis techniques employed to extract meaningful insights into the sensing behavior of the nanoparticles.

The experimental details provided in this chapter serve as a foundation for the subsequent chapters, where we present the results and discussions based on the CO_2 sensing measurements conducted on $BaTiO_3$ nanoparticles. The accurate and precise execution of the experimental procedures ensures the reliability and validity of our findings, contributing to the advancement of CO_2 sensing technology using nanostructured materials.

3.1. Material Synthesis

The most simple and cost effective method for obtaining nanoparticles is mechanical milling of bulk materials. We have adopted the method of Planetary ball milling for obtaining the nanoparticles. It is a variant of high energy mechanical milling. There are several types of mechanical milling methods that can be employed for the synthesis and processing of materials. The choice of the specific method depends on the desired outcome, the type of material being milled, and the available equipment. Here are some common types of mechanical milling techniques:

Ball Milling: Ball milling is one of the most widely used methods for mechanical milling. It involves the use of a rotating container filled with grinding balls, where the materials to be milled are placed. The high-energy impacts between the balls and the materials result in the fracturing and refinement of the particles. Ball milling is suitable for both dry and wet milling processes.

Planetary Milling: Planetary milling is a variant of ball milling that involves the use of planetary ball mills. In this technique, the grinding balls are mounted on a rotating plate or vials that rotate around their own axis while also rotating around a central axis. This dual rotation creates a highly energetic milling environment, leading to efficient milling and mixing of the materials.

Vibratory Milling: Vibratory milling utilizes vibrating containers or tubes to achieve mechanical milling. The container or tube is subjected to vibrations or oscillations, which cause the materials to be milled to impact against each other and the walls of the container. This movement leads to the breakdown and refinement of the particles.

Attrition Milling: Attrition milling involves the use of milling media, such as grinding balls or rods, that move within a container or chamber. The materials to be milled are placed in the chamber, and the collision and friction between the milling media and the materials result in particle size reduction. Attrition milling is particularly suitable for fine and ultrafine milling processes.

High-Energy Milling: High-energy milling refers to mechanical milling techniques that involve high energy inputs. These methods typically use specialized milling equipment, such as high-energy ball mills or attritor mills, which provide higher impact forces and milling intensities. High-energy milling is effective for achieving rapid milling and refining of materials.

Jet Milling: Jet milling utilizes high-speed jets of gas, such as compressed air or nitrogen, to cause particle-particle and particle-wall collisions. The materials to be milled are introduced into the milling chamber, and the high-velocity gas jets create turbulent conditions that result in particle size reduction. Jet milling is suitable for micronization and fine milling of materials.

Planetary ball milling is a suitable choice for synthesizing barium titanate ($BaTiO_3$) nanoparticles due to several advantages it offers. Here are some reasons why planetary milling can be preferred for $BaTiO_3$ nanoparticle synthesis:

Efficient Mixing and Grinding: Planetary milling provides highly efficient mixing and grinding of materials. The rotation of the planetary ball mill and the simultaneous rotation of the grinding jars create a strong centrifugal force and impact energy. This leads to intense collisions between the grinding balls and the $BaTiO_3$ precursor powders,

resulting in effective mixing and grinding. Efficient mixing is crucial for achieving homogeneity in the precursor mixture, ensuring uniform distribution of elements and a consistent composition in the synthesized nanoparticles.

Controlled Size Reduction: Planetary milling allows for controlled size reduction of the $BaTiO_3$ particles. By adjusting the milling parameters such as milling time, rotational speed, and ball-to-powder ratio, one can tailor the particle size distribution to the desired range, including the nanoscale. This control over particle size is essential for tuning the properties of the $BaTiO_3$ nanoparticles and achieving specific functionalities.

High Energy Input: Planetary ball mills provide high energy input due to the combination of rotational and vibrational movements. The high impact forces generated during milling facilitate the fracture and refinement of the $BaTiO_3$ particles. This promotes the formation of smaller crystallites and enhances the reactivity of the particles, leading to the synthesis of fine and highly reactive $BaTiO_3$ nanoparticles.

Scalability: Planetary milling is a scalable technique that can be easily adapted for large-scale production. The use of multiple grinding jars in a planetary ball mill allows for simultaneous milling of multiple samples, increasing the throughput. This makes planetary milling suitable for both laboratory-scale research and industrial-scale synthesis of $BaTiO_3$ nanoparticles.

Control over Milling Environment: Planetary ball mills allow for control over the milling environment, such as the milling atmosphere and temperature. The milling atmosphere can be adjusted by choosing appropriate milling jars and sealing options. Additionally, the milling temperature can be controlled by cooling systems. These capabilities enable the synthesis of $BaTiO_3$ nanoparticles under specific conditions, enhancing the control over the final properties of the nanoparticles.

Versatility: Planetary milling is a versatile technique that can be used for various materials, including ceramics, metals, and composites. This versatility allows for the synthesis of $BaTiO_3$ nanoparticles with different compositions, doping elements, and morphologies, expanding the range of potential applications.

Thus, planetary milling offers efficient mixing and grinding, controlled size reduction, high energy input, scalability, control over milling environment, and versatility, making it a suitable choice for synthesizing $BaTiO_3$ nanoparticles. These advantages contribute to the production of well-dispersed, fine, and highly reactive $BaTiO_3$ nanoparticles with tunable properties for applications in electronics, catalysis, sensors, and energy storage.

In our experiments, Commercially available Barium Titanate(BT) powder (Sigma-Aldrich, 208108-500G) was considered for milling in order to reduce its particle size using three Tungstun Carbide (WC) grinding balls (diameter 20 mm each) in a planetary monomill (PULVERISETTE 6, FRITSCH, Germany) having WC grinding bowl capacity of 80 mL. Prior to milling the bowl and balls were cleaned by keeping it filled with Acetone for few hours, followed by milling of Silicon Carbide powder(Alfa Aesar, coarse, 46 grit), half-filled in grinding bowl for 20 hours at 200 rpm.

Figure 3.1 PULVERISETTE 6, FRITSCH, Germany, planetary monomill system.

The BT powder was milled for 100 hours at 250 rpm in multiple cycles of 15 minutes in order to control the temperature of the sample and also, to scrape the powder that sticks to the inner walls of the grinding bowl(figure3.1). The whole process was conducted at normal atmospheric conditions. Nano-BT powders were taken out in small quantities at various intervals during milling. As a pellet binder, few drops of 2% w/v aqueous solution of Polyvinyl alcohol (PVA; SDFCL, 39791 KO5) were added to nano-BT samples taken in a mortar and pestle, and the mixture was ground for about 10 minutes. The contents were then filled into hydraulic punch-die cylindrical pellet mold (diameter = 10 mm). It was pressed with a force upto 20 kN for few minutes under a hydraulic press machine (figure 3.2) to obtain nano-BT pellets.

Figure 3.2 Pellet mold set with mortar and pestle; and the hydraulic press used in this study.

3.2. Material Characterization

Nano-BT obtained by dry ball milling was characterized using X-ray diffraction (XRD), Field Emission Scanning Electron Microscopy (FESEM), Transmission Electron Microscopy (TEM), Energy-dispersive X-ray Spectroscopy (EDX), and Impedance Analyzer. These characterization techniques provide comprehensive insights into the structural, morphological, elemental, and electrical properties of the nano-BT sample.

The X-ray diffractograms were generated for the nano-BT powder sample with the help of line broadening measurements using X-ray diffraction on a Rigaku Ultima IV, multipurpose X-Ray Diffraction system(figure 3.3) using Ni filtered Cu-Kα radiation generated at 40 kV, 30 mA. Parameters used for the XRD were, scan range: 5º to 90º, sampling width: 0.02º and scan speed: 3º /min.

XRD is a widely used characterization technique in the field of materials science and nanotechnology. It is employed to investigate the crystal structure, phase composition, and

***Figure* 3.3 Rigaku Ultima IV, multipurpose X-Ray Diffraction system; inside view (inset)**

crystallite size of various materials, including nanostructured materials like Barium Titanate ($BaTiO_3$). XRD relies on the interaction of X-rays with the crystalline lattice of a material. When X-rays are incident on a crystalline sample, they undergo constructive and destructive interference as they interact with the crystal planes. The resulting diffraction pattern provides information about the arrangement of atoms in the crystal and allows for the determination of crystallographic parameters. The XRD pattern obtained provides valuable information about the crystal structure and phase composition of the BT nanoparticles. By analyzing the positions and intensities of the diffraction peaks in the pattern, the crystallographic phases present in the sample can be identified. In the case of nano-BT, the diffraction pattern can reveal the presence of the desired perovskite phase and potential secondary phases.

XRD pattern were generated for BT powder samples collected at different time intervals during the milling process, specifically at 0, 25, 50, 75, and 100 hours, and analyzed with X'pert HighScore Plus and X'pert Organizer softwares. These software tools are commonly employed for XRD data analysis and offer features such as crystallographic phase identification, refinement, and comparison with reference databases such as CIF (Crystallographic Information File) and NIST (National Institute of Standards and Technology) data. These analyses allow for the determination of crystal structure, phase composition, and any changes occurring in the BT powder during the milling process. The obtained parameters were used with Scherrer formula given below to calculate the crystallite size and lattice strain.

Crystallite size = $k\lambda / (\beta \cos \theta)$

Where:

k is the shape factor, which depends on the particle morphology. In this study, a value of 0.89, commonly used for spherical particles, was considered.

λ is the X-ray wavelength, which was taken as 1.54178 Å, corresponding to the Cu-Kα radiation used in the XRD analysis.

β is the structural broadening, which is determined by the full width at half maximum (FWHM) of the diffraction peak. It represents the extent of crystallographic imperfections, such as lattice strain or microstrain.

θ is the Bragg angle, which is the angle between the incident X-ray beam and the crystal planes that satisfy the Bragg's law for constructive interference.

By applying the Scherrer formula to the XRD data, the crystallite size of the nano-BT particles was determined. This information is essential as it provides insights into the size-dependent properties and the potential application of the nanoparticles.

Additionally, the XRD (X-ray diffraction) diffractograms of the nano barium titanate powder, which was obtained through a ball milling process lasting for 100 hours, were analyzed using Reitveld refinement. Reitveld refinement is a technique used to extract precise structural information from XRD data. The X'pert High Score Plus and X'pert Organiser software packages were employed for the refinement process. These software tools offer advanced features and algorithms specifically designed for XRD analysis and refinement. During the refinement, CIF (Crystallographic Information File) and NIST (National Institute of Standards and Technology) data were included. CIF files contain detailed information about the crystal structure, lattice parameters, and atomic

positions of a material. NIST data, on the other hand, provides reference data for comparison and validation purposes.

Field Emission Scanning Electron Microscopy (FESEM) is a powerful characterization technique used to investigate the surface morphology and microstructure of materials, including the milled Barium Titanate (BT) nanoparticles in this study. FESEM provides high-resolution imaging and detailed information about the sample's topography, particle size, shape, and distribution.

FESEM operates on the principle of electron imaging. A focused beam of electrons is scanned across the surface of the sample, and the interactions between the electrons and the sample produce various signals that can be detected and analyzed. These signals include secondary electrons (SE), backscattered electrons (BSE), and characteristic X-rays. SEs are low-energy electrons emitted from the surface, while BSEs are higher-energy electrons that are backscattered from the sample due to interactions with the atomic nuclei. These signals are detected and used to generate high-resolution images of the sample.

FESEM offers several advantages for the characterization of milled BT nanoparticles. One of the key advantages of FESEM is its high spatial resolution, which allows for detailed imaging and analysis of the sample's surface features. With advanced detectors and imaging techniques, FESEM can achieve sub-nanometer resolution, enabling the visualization of fine surface details and the examination of individual nanoparticles or microstructures. The use of FESEM in this study enables the examination of the morphology of the milled BT particles, including their size, shape, and surface roughness. It also allows for the observation of particle size reduction, shape modifications, agglomeration tendencies, and the overall distribution of the milled BT particles.
FESEM analysis was further complemented by the use of Energy-dispersive X-ray Spectroscopy (EDX). EDX is an analytical technique that is integrated into the FESEM system, enabling the elemental analysis of the sample. By analyzing the energy and intensity of these X-rays, the elemental composition of the milled BT nanoparticles can be determined. This information is valuable for confirming the presence of desired elements and assessing any impurities or contaminants in the sample.

FESEM with EDX provides a comprehensive understanding of the surface morphology and elemental composition of the milled BT nanoparticles. It complements the information obtained through X-ray diffraction (XRD) analysis by offering detailed visualization and elemental mapping. The obtained images provide valuable insights into the particle size, shape, and distribution, while the elemental analysis facilitate the identification and mapping of the chemical elements present in the sample.

In this study, morphology of nano-BT powder was characterised by Field Emission Scanning Electron Microscopy (SIGMA ZEISS, Supra 35 VP, 30kV, Image Resolution-1.5 nm, Energy Resolution~133 eV) and quantitative elemental analysis was done using Energy Dispersive X-ray spectroscopy (EDX).

Transmission Electron Microscopy (TEM) is an advanced imaging technique that provides exceptional resolution and allows for the direct visualization of materials at the atomic scale. It is an indispensable tool for the characterization of the milled Barium Titanate (BT) nanoparticles in this study, offering valuable insights into their microstructure, crystallography, defects, and elemental composition.

In TEM, a focused electron beam is transmitted through an ultra-thin specimen, typically less than 200 nanometers thick. The interaction of the electrons with the atoms in the sample generates different types of signals, including elastic scattering, inelastic scattering, and electron diffraction. These signals are collected and processed to generate images and diffraction patterns that reveal detailed information about the sample's structure.

TEM allows for the observation of various imaging modes, each providing unique insights into the milled BT nanoparticles. Bright-field imaging is commonly used for visualizing the overall morphology, size, and shape of the nanoparticles. It relies on the contrast generated by differences in electron density within the sample. This mode is useful for assessing the uniformity of particle size and shape distribution.

Bright-field imaging is a commonly used imaging mode in Transmission Electron Microscopy (TEM) that provides valuable information about the overall morphology, size, and shape of the milled Barium Titanate (BT) nanoparticles. In this mode, a highly focused electron beam is transmitted through the sample, and the electrons that pass through interact with the atoms and are detected to form an image. The contrast in the resulting image is primarily determined by variations in electron scattering and absorption within the sample.

Bright-field images reveal the distribution and arrangement of the milled BT nanoparticles within the sample. The nanoparticles appear as bright regions against a darker background, allowing for the visualization of their size, shape, and spatial distribution. By examining a series of bright-field images at different magnifications, it is possible to assess the uniformity of particle size and shape distribution.

This imaging mode provides valuable insights into the morphology of the milled BT nanoparticles. It allows for the determination of parameters such as particle size, aspect ratio, and surface features. By observing the shape and surface characteristics of the nanoparticles, it is possible to gain insights into their growth mechanisms, aggregation behavior, and surface modifications.

Bright-field imaging is often used in conjunction with other TEM techniques, such as high-resolution imaging and selected area diffraction (SAD), to provide a comprehensive understanding of the milled BT nanoparticles. For example, bright-field images can be combined with high-resolution images to correlate the overall morphology of the nanoparticles with the atomic-scale structure.

Dark-field imaging is an essential technique in Transmission Electron Microscopy (TEM) that provides valuable information about crystal defects, strain, and lattice

distortions within the milled Barium Titanate (BT) nanoparticles. It offers a unique contrast mechanism that selectively scatters and diffracts electrons from specific crystal planes or regions of interest.

In dark-field imaging, a specific set of diffracted electrons is selected by inserting an aperture or objective aperture in the TEM system. This aperture blocks the direct beam and allows only the diffracted electrons to pass through, creating a dark background in the image. The diffracted electrons originate from specific crystal planes that satisfy the Bragg condition, resulting in constructive interference and enhanced scattering.

Dark-field images highlight crystal defects and strained regions as bright spots against a dark background. These bright spots correspond to areas where the diffracted electrons are redirected towards the detector due to the presence of lattice imperfections. Crystal defects such as dislocations, stacking faults, and vacancies can be visualized and characterized using dark-field imaging.

By analyzing dark-field images, valuable information about the density and distribution of crystal defects within the milled BT nanoparticles can be obtained. The size, shape, and arrangement of these defects can provide insights into the mechanical, electrical, and optical properties of the nanoparticles. Additionally, dark-field imaging can reveal the presence of strain fields or lattice distortions caused by external factors or the milling process itself.

Dark-field imaging is often combined with other techniques, such as bright-field imaging and selected area diffraction (SAD), to provide a comprehensive understanding of the structural properties of the milled BT nanoparticles. Bright-field imaging provides an overall view of the nanoparticle morphology, while dark-field imaging focuses on specific crystal planes and defects. SAD analysis can further confirm the crystal structure and orientation of the nanoparticles.

High-resolution TEM (HRTEM) is an essential technique for investigating the atomic structure and lattice arrangement of materials. It provides detailed images of lattice fringes, enabling the determination of crystallographic information such as interplanar spacing, crystal orientation, and the presence of point defects. HRTEM allows for the precise characterization of the milled Barium Titanate (BT) nanoparticles in this study, providing insights into their atomic ordering, crystal defects, phase composition and interfacial phenomena.

HRTEM employs a highly focused electron beam that interacts with the sample at a high spatial resolution. The resulting transmitted electrons form an image on a specialized detector, which is capable of capturing the intricate details of the sample's atomic structure. Unlike conventional TEM, HRTEM offers improved spatial resolution, allowing for the direct visualization of lattice fringes and individual atomic columns.

The lattice fringes observed in HRTEM images correspond to the parallel atomic planes within the crystal lattice of the milled BT nanoparticles. These fringes appear as lines

or patterns, representing the arrangement of atoms and their interatomic distances. By analyzing the spacing and orientation of these lattice fringes, valuable crystallographic information such as crystal planes, crystal defects, and crystallographic ordering can be determined.

HRTEM is particularly effective for studying the nanoscale features of materials, including grain boundaries, dislocations, stacking faults, and surface structures. These features significantly influence the properties and behavior of the milled BT nanoparticles. HRTEM allows for the direct observation and characterization of these features, aiding in the understanding of their impact on CO_2 sensing characteristics.

Additionally, HRTEM provides insights into interfacial phenomena, such as epitaxial growth and interface structure. The atomic-scale visualization of interfaces between different phases or materials enables the examination of their atomic arrangement and potential interfacial defects. This information is crucial for understanding the interfaces within the milled BT nanoparticles and their role in CO_2 sensing behavior.

EDX analysis, which can be integrated with TEM, provides elemental composition information. By capturing X-rays emitted from the sample when bombarded by the electron beam, EDX enables the identification and quantification of elements present within the milled BT nanoparticles. This analysis is crucial for confirming the desired elemental composition and assessing any impurities or contaminants.

In addition to the imaging capabilities of TEM, Transmission Electron Microscopy also allows for the analysis of the crystal structure of materials through Selected Area Diffraction (SAD) patterns. SAD is a technique employed to obtain detailed information about the arrangement of atoms in a sample at the nanoscale.
SAD involves the selection of a specific area of the specimen, typically a few nanometers in diameter, which is then illuminated with a highly converged electron beam. The selected area is typically chosen to contain a single crystal or a specific region of interest within a polycrystalline material. The electron beam interacts with the crystal lattice and undergoes elastic scattering, resulting in the formation of a diffraction pattern. The diffraction pattern is recorded on a specialized detector and provides information about the crystallographic orientation, lattice spacing, and symmetry of the sample.

The diffraction patterns obtained from SAD provide valuable information about the crystal structure, lattice spacing, crystallographic orientations, and the presence of defects in the milled BT nanoparticles. The patterns consist of a series of concentric rings or spots that correspond to the diffraction of the electron beam by different crystal planes within the sample. These diffraction patterns can be recorded on a phosphor screen or a detector, and they can be further analyzed to extract important crystallographic information.

By applying techniques such as Fourier transformation and indexing, the diffraction patterns obtained from SAD can be used to determine the crystal symmetry, lattice parameters, and the orientation relationship between different grains or phases within

the milled BT nanoparticles. SAD is particularly useful in identifying the crystallographic phases present in the sample, confirming the desired nano-BT perovskite structure, and assessing the degree of crystallinity and crystal quality.

SAD analysis was performed in combination with TEM imaging techniques, allowing for the simultaneous examination of the sample's microstructure and crystallographic information. This integration provides a comprehensive understanding of the milled BT nanoparticles, including their crystal structure, morphology, size distribution, and orientation relationships.

Energy-Dispersive X-ray Spectroscopy (EDX or EDAX) is a valuable analytical technique that is commonly used in conjunction with Transmission Electron Microscopy (TEM) to provide elemental composition information of the milled Barium Titanate (BT) nanoparticles. It enables the identification and quantification of the elements present within the nanoparticles and offers insights into their chemical composition and elemental distribution.

EDX is based on the principle that when a material is bombarded with high-energy electrons, it emits characteristic X-rays that are specific to the elements present. In TEM, an EDX detector is used to collect these emitted X-rays, and their energy spectra are analyzed to determine the elemental composition.

The EDX detector captures the X-rays emitted by the milled BT nanoparticles, and the resulting spectrum provides information about the elements present and their relative abundances. By comparing the energy peaks in the spectrum to known X-ray energy signatures of different elements, the composition of the nanoparticles can be determined.
EDX allows for both qualitative and quantitative analysis. Qualitative analysis identifies the elements present within the nanoparticles, while quantitative analysis measures the elemental composition and provides information about the relative atomic percentages of the detected elements. This information is crucial for understanding the chemical makeup of the nanoparticles and how it relates to their CO2 sensing properties.

In addition to elemental composition analysis, EDX can also provide elemental mapping information. By scanning the electron beam across the sample, the EDX detector can collect X-ray spectra at each point. This data can then be used to generate elemental maps, which visually represent the distribution of different elements within the nanoparticles. Elemental mapping provides insights into the spatial arrangement and segregation of elements, helping to understand the nanoscale chemistry of the milled BT nanoparticles.

EDX analysis within TEM offers several advantages. It provides localized elemental information, allowing for the characterization of specific regions or features within the nanoparticles. It is a non-destructive technique, enabling the analysis of the same sample region before and after other TEM imaging or spectroscopic experiments. Furthermore, EDX analysis can be performed simultaneously with other TEM techniques, such as high-resolution imaging and electron diffraction, providing a

comprehensive understanding of the structural and elemental properties of the nanoparticles.

Finally, the impedance spectrometry technique is employed to study the electrical properties of the nanostructured Barium Titanate (nano-BT) material. The measurements are typically performed using specialized equipment, such as an impedance analyzer or a frequency response analyzer. Impedance spectrometry is a technique used to measure the electrical impedance of a material or device as a function of frequency. It provides information about the electrical properties and behavior of the material, particularly in the context of electrical conductivity and capacitance. The impedance spectrometry measurements involve applying an AC voltage signal across the material and measuring the resulting current response. The AC voltage signal is varied over a range of frequencies, typically spanning from a few hertz to several megahertz. The obtained impedance data is then analyzed to extract key parameters such as impedance magnitude, phase angle, and impedance spectroscopy plots. These parameters can provide insights into the electrical conductivity, dielectric properties, and charge storage behavior of the nano-BT material.

By conducting impedance spectrometry on the nano-BT material, we can assess its suitability for gas sensing applications, as impedance changes in the presence of a target gas (such as carbon dioxide) can indicate its sensing capabilities. The measurements help evaluate the sensitivity, response time, and selectivity of the nano-BT gas sensor.
Wayne Kerr 6500B Precision Impedance Analyzer was utilized in this study for AC measureents. It was used in parallel mode with a 1-volt AC supply and a frequency range of 50 Hz to 1 MHz for impedance spectrometry of nano-BT pellets. This allows

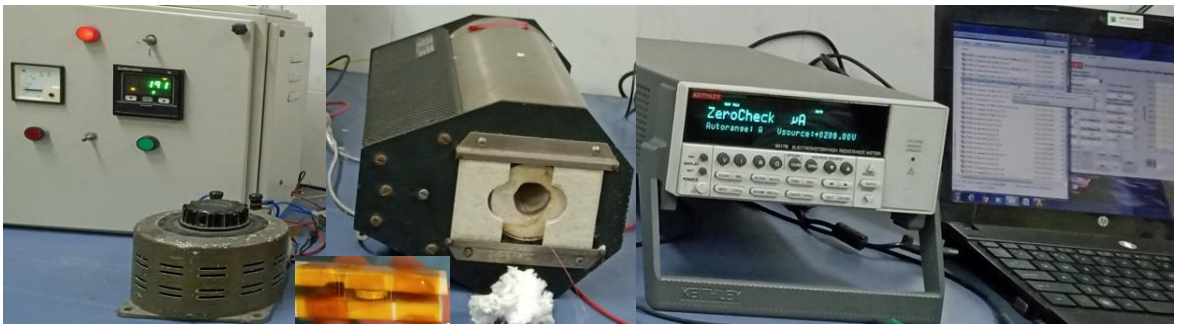

Figure 3.4 Keithley 6517B Electrometer/ High Resistance Meter and Furnace system (0.48kW).

for detailed characterization of the electrical properties of the nano-BT material. It enables the analysis of impedance changes at different frequencies and provides insights into the material's conductivity, capacitance, and other relevant electrical parameters. These measurements can contribute to understanding the material's gas sensing capabilities and its potential for carbon dioxide detection.
DC measurements at varying temperatures was carried out with Keithley 6517B Electrometer/ High Resistance Meter and Furnace system (0.48kW) capable upto 1100 ºC, fitted with thermo-stat and variac(figure 3.4). It is a significant instrument, particularly for applications involving low currents and high resistances. Its high sensitivity, accuracy, and versatile measurement capabilities make it an invaluable tool.

Chapter 4
Synthesis And Characterization of nanostructured $BaTiO_3$

This chapter serves as a comprehensive analysis of the experimental findings and their implications. The subsequent sections delve into the detailed results obtained from the synthesis of nano-BT powder, microstructural characterization results of the nano-BT material using advanced techniques like Field Emission Scanning Electron Microscopy (FESEM), Transmission Electron Microscopy (TEM), and Energy-Dispersive X-ray Spectroscopy (EDX). These techniques provide insights into the morphology, microstructure, and elemental composition of the nano-BT particles. Additionally, the chapter covers the results of impedance spectrometry measurements and the resulting sensing characteristics of the nano-BT material. The electrical properties and gas-sensing performance of the nano-BT material are evaluated and analyzed in detail. Finally, the chapter concludes with a comprehensive discussion and interpretation of the results. The implications and potential applications of the synthesized nano-BT material as a gas sensor, particularly for carbon dioxide detection, are thoroughly examined in the next chapter.

Overall, this chapter serves as a pivotal section of the study, presenting the results of the synthesis and characterization efforts and providing an in-depth discussion of their significance in the context of nano-BT's properties and potential applications.

4.1 Synthesis of nano-BT powder and its structural characterization

The X-ray diffractograms for as synthesised nano-BT powder at different milling hours are shown in figure 4.1. With incremental milling hours, XRD depicts shortening and broadening of intensity peaks. This signifies continuous reduction in particle size and generation of lattice strain in BT due to milling. With continuous ball milling, XRD

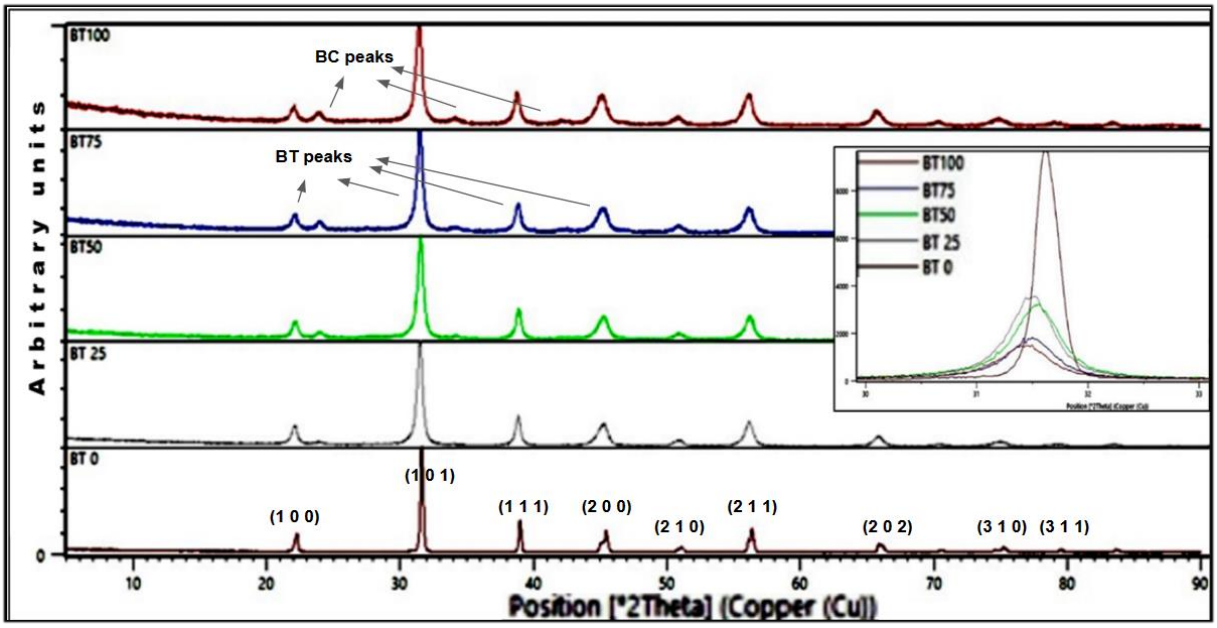

Figure 4.1 X-ray Diffractometer 2D plots (main) of BT unmilled (BT 0) and milled for 25 hours (BT 25), 50 hours (BT50), 75 hours (BT75) and 100 hours (BT100); and comparative, highest peaks (inset).

peaks become broader and less intense because the crystallographic planes responsible

for the diffraction are no longer perfectly aligned, and the X-rays are scattered over a wider range of angles.
Additionally, following conclusions can be drawn from the XRD diffractograms:

- All the XRD peaks of BT 0 graph denote the characteristic peaks of pure Barium Titanate: The XRD graph for the initial sample, labeled as BT 0, shows distinct peaks that correspond to the crystal structure of pure Barium Titanate. These peaks are characteristic of BT and indicate the presence of BT as the primary phase in the sample.
- Other graphs (BT 25 - BT 100) contain extra peaks corresponding to Barium Carbonate (BC): In contrast to the BT 0 graph, the XRD graphs for samples labeled as BT 25, BT 50, BT 75, and BT 100 show additional peaks that correspond to a different compound called Barium Carbonate (BC). These peaks indicate the presence of BC as an impurity or secondary phase in the samples.
- The presence of BC peaks is caused by the absorption of CO_2 into BT nanoparticles: The reason for the appearance of BC peaks in the XRD graphs is attributed to the absorption of carbon dioxide into the nanoparticles of Barium Titanate during the milling process. The CO_2 comes from the surrounding environment during the milling operation.
- BC peaks increase in height compared to BT peaks as milling hours increase: it is observed that the intensity or height of the BC peaks progressively increases as the milling hours increase (BT 25 to BT 100 graphs). This indicates that the concentration of Barium Carbonate relative to Barium Titanate increases due to increase in rate of absorption of CO_2 in BT at smaller particle sizes.

The crystallite sizes of as synthesised nano-BT powder have been found to be in the range of 20 nm to 40 nm (refer to Table 4.1) as calculated using Scherrer formula described in the previous chapter.

Milling time (in hour)	Crystallite size (in nm)	Lattice strain (%)
0	118.0	0.262
25	28.0	0.607
50	25.7	0.714
75	24.9	0.731
100	22.9	0.781

Table 4.1 Comparision of BT nanoparticles particles obtained from planetary ball milling at various milling hours. At 0 hours, the commercially available BT is unmilled, in its original form.

As the milling hours increase, the barium titanate particles undergo continuous mechanical impact, abrasion, and fracturing. These processes lead to a reduction in particle size. With prolonged milling, the average particle size of barium titanate can be reduced to the nanoscale, typically below 100 nanometers. This leads to a broader and shorter XRD peak shape, indicating a reduction in particle size and the presence of smaller crystalline domains. The broadening is a consequence of the increased distribution of lattice strains and defects caused by the milling process. This reduction in particle size is desirable in many applications because it can enhance the material's properties, such as increased surface area, improved reactivity, and altered electronic and optical properties.

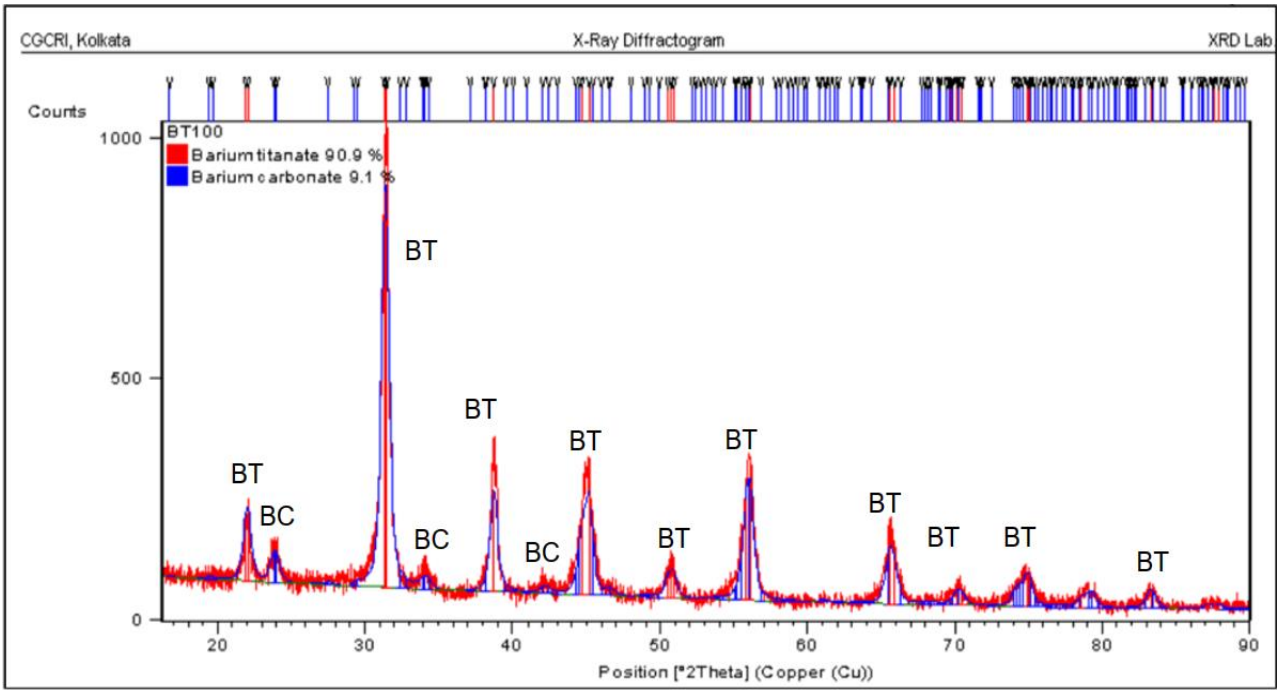

Figure 4.2 Reitveld refinement of X-ray Diffractometer 2D plots of 100 hour milled nano-BT

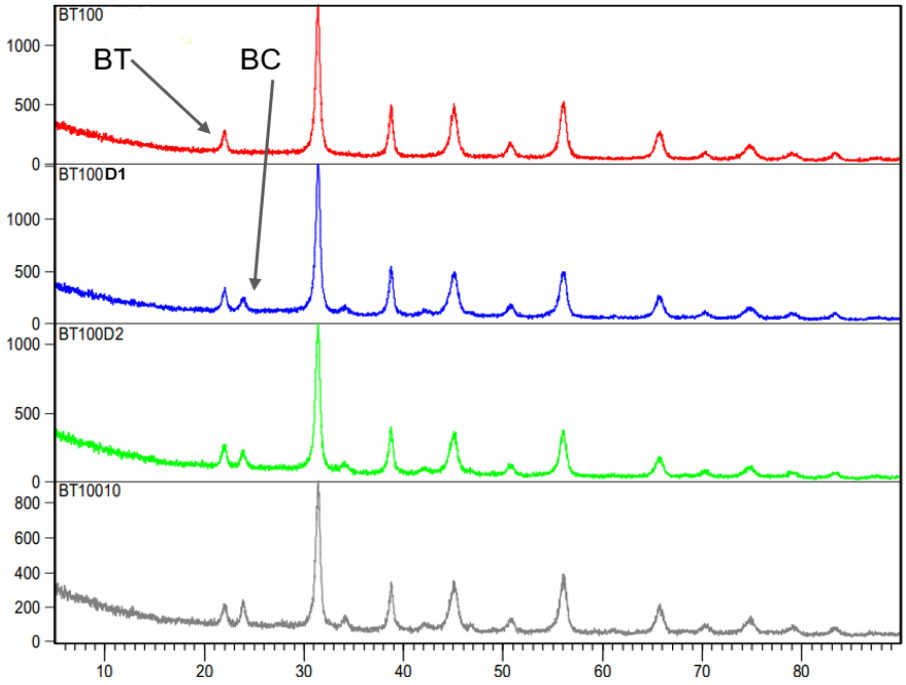

Figure 4.3 X-ray Diffractometer 2D plots of 100 hour milled nano-BT over multiple days(BT100= just after milling, BT100D1=after 1 day of milling and so on).

The XRD diffractograms of nano barium titanate (nano-BT) powder prepared through ball milling process lasting for 100 hours, was subjected to Reitveld refinement using X'pert High Score Plus and X'pert Organiser softwares, with the inclusion of CIF and NIST data.

The refinement process aimed to obtain accurate structural and compositional information about the material. From the refinement, it was observed that the nano barium titanate material absorbed approximately 9.1% of barium carbonate (figure 4.2) within one day after milling. This absorption indicates the incorporation of barium carbonate into the structure of the nano barium titanate, potentially leading to changes in its properties and behavior. Figure 4.3 shows how XRD graphs of 100 hour milled nano-BT over multiple days after milling differ in Barium Carbonate(BC) peaks. These increamental BC peaks indicate absorption of CO_2 in nano-BT.

By utilizing Reitveld refinement and incorporating CIF and NIST data, the diffractograms of the nano barium titanate powder were carefully analyzed and fitted to obtain accurate information about its crystal structure, phase composition (table 4.2), lattice parameters, and atomic positions.

BT100	DAY 1	DAY2	DAY10
BT%	90.9	89.7	86.4
BC%	9.1	10.3	13.6
CO_2%	2.029	2.297	3.032

Table 4.2 Absorption of CO_2 in BT nanoparticles to form Barium Carbonate(BC) over many days after 100 hours of ball milling.

This allowed for a comprehensive understanding of the material's properties and characteristics at the atomic scale. Reitveld refinement is a sophisticated method that involves fitting the experimental XRD data with a structural model to obtain precise crystallographic information.

4.2. Microstructural characterisation: FESEM, TEM and EDX

The electron images obtained from FESEM describing the morphology of the 100 hour milled nano-BT particles are shown in figure 4.4. Mostly in spherical shape, and size varying between 15 nm to 40 nm, BT nanoparticles are found to be agglomerated due to their high surface energy.

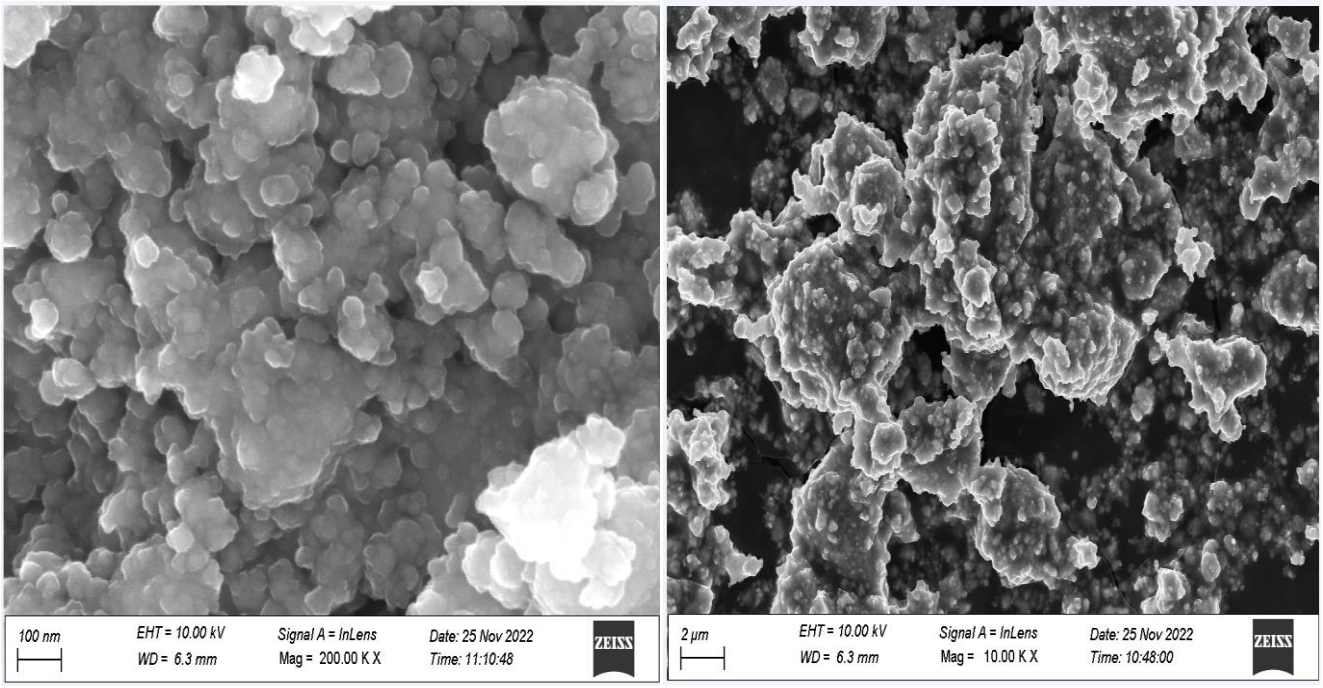

Figure 4.4 Field-emission scanning electron microscopy (FE-SEM) photomicrographs of 100 hours milled Barium Titanate ($BaTiO_3$) nanoparticles(BT100) at higher nano resolution (left) and at the micro-scale (right).

Energy Dispersive X-ray spectroscopy (EDX) graphs for quantitative analysis in figure 4.5, describes the elemental composition of the 100 hours milled (BT100) Barium

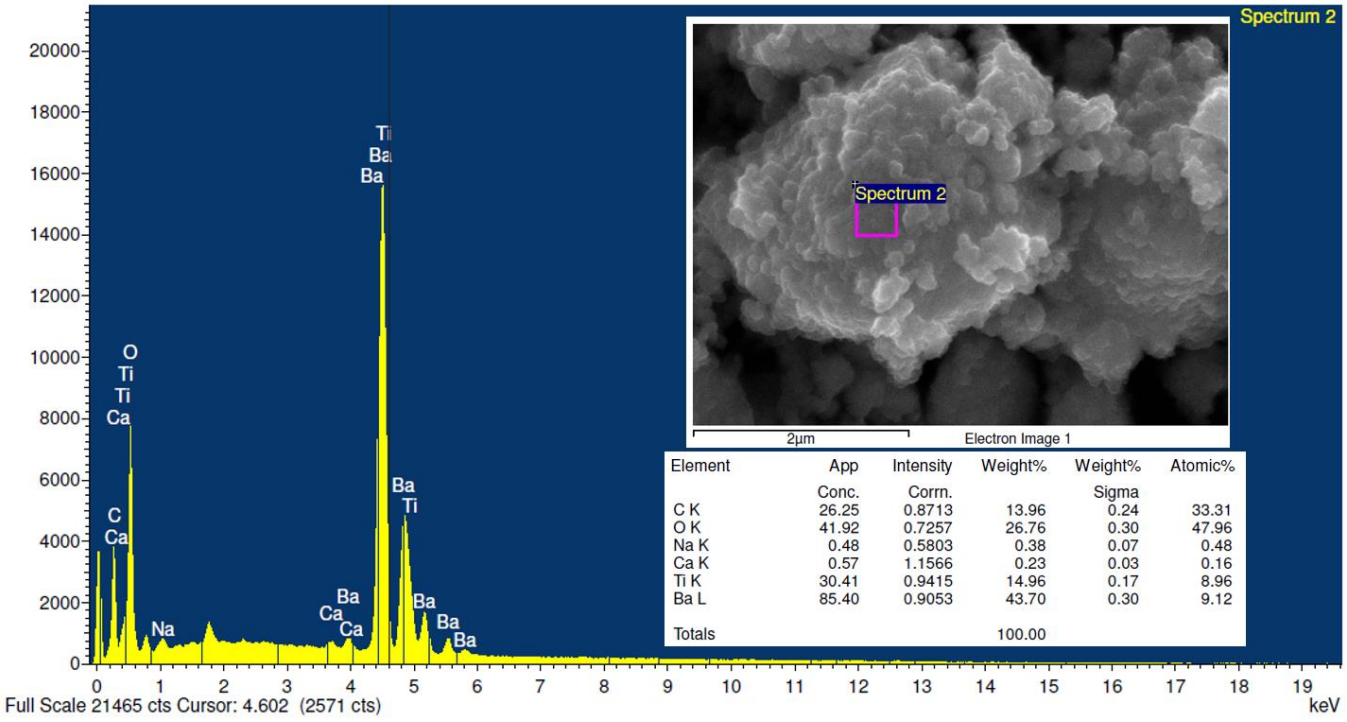

Figure 4.5 Energy Dispersive X-ray spectroscopy (EDX) graphs of 100 hour milled barium titanate (BT100) powder sample.

Titanate ($BaTiO_3$) nanoparticles. The graph displays the intensity of X-ray peaks corresponding to different elements present in the sample. The X-axis represents the energy levels of the detected X-rays, while the Y-axis represents the intensity or count of X-rays.Upon analysis of the EDX graph, several prominent peaks can be observed. The peak corresponding to carbon (C), indicates the presence of carbon compound. Significant carbon percentage confirms presence of Barium Carbonate. There are no peaks of Tungsten, as the ball milling container made of Tungsten Carbide, which removes any possibility of Carbon coming from the container. This is also in conformity with the carbon composition obtained from Rietveld refinement of the XRD data. Other significant peaks of Barium, Titanium and Oxygen are evident. It is worth noting that EDX is basically a qualitative technique, providing information about the elemental composition rather than precise quantitative measurements.

Therefore, the relative intensities of the obtained peaks give an indication of the elemental distribution within the sample.The transmission electron microscopy (TEM) images in figure 4.6 describes the microstructure, grain size, grain boundaries, crystal planes etc of BT100 sample. The bright-field image (figure 4.6a) cleary displays almost spherical nano-BT particles of about 20 nm in diameter. Individual particles are visible as bright whereas agglomerated particles are darker in appearance. An embedded grain of Barium Carbonate in BT with distinct grain boundary is clearly visible in high resolution TEM image (figure 4.6b). The reduced Fast Fourier Transform (FFT) of a high-resolution (HR) image (figure 4.6c) refers to the transformation of the electron image from the spatial domain to the frequency domain using the FFT algorithm while reducing the size or resolution of the resulting frequency spectrum. The Selected Area Diffraction (SAD) image (figure 4.6d) appears as a collection of bright diffraction spots

arranged in a circular pattern against a dark background. The spots exhibit various sizes and intensities, representing the diffracted electrons scattered by different crystal planes within the sample. The SAD pattern establishes that the sample has a crystal structure

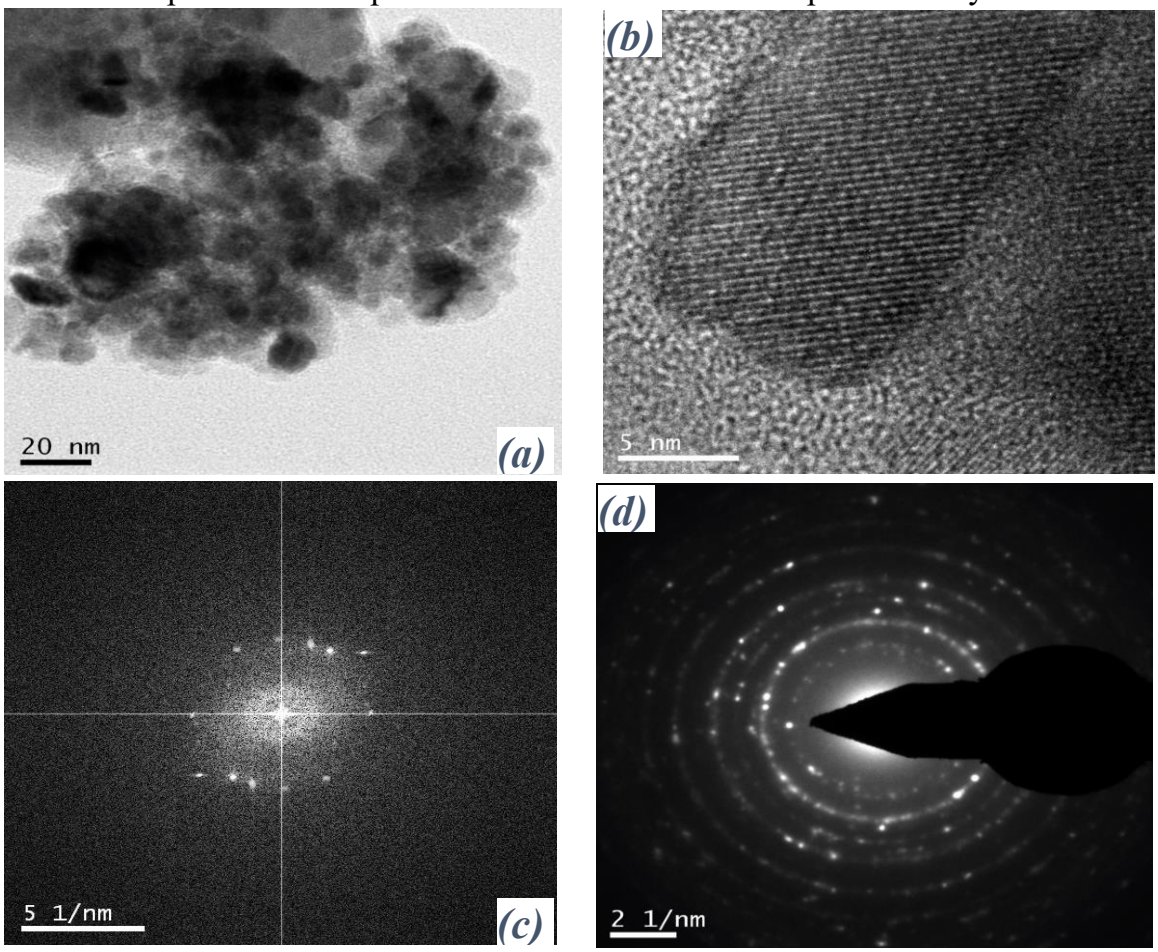

Figure 4.6 TEM images: (a)BF (b)HRTEM (c)Reduced FFT of HR and (d)SAD images of BT100

of BT. Distinct diffraction spots correspond to specific crystallographic planes providing information about the lattice spacing and orientation of the copper grains. Observed diffraction spots are compared the with known crystallographic data, and the SAD pattern are indexed, confirming the presence of BT. The Miller indices of the diffraction spots are determined, enabling the determination of crystallographic orientations within the sample.

Energy-Dispersive X-ray Spectroscopy(EDX) is a technique used to analyze the elemental composition of materials at the nanoscale by detecting characteristic X-rays emitted when a sample is irradiated with a focused electron beam. Elemental composition of nano-BT is visible in figure 4.7. The EDX image shows the presence of three main elements: Ba, Ti and O. Significant Carbon peak suggests absorbed CO_2 into the nano-BT. Cu peak is due to the sample grit made of copper used to mount the sample. The multiple peaks observed for Ba element in the EDX spectrum can be attributed to various factors, such as different X-ray emission lines, scattering effects, absorption etc. These factors influence the energy distribution and intensity of the emitted X-rays, leading to the observation of multiple peaks.

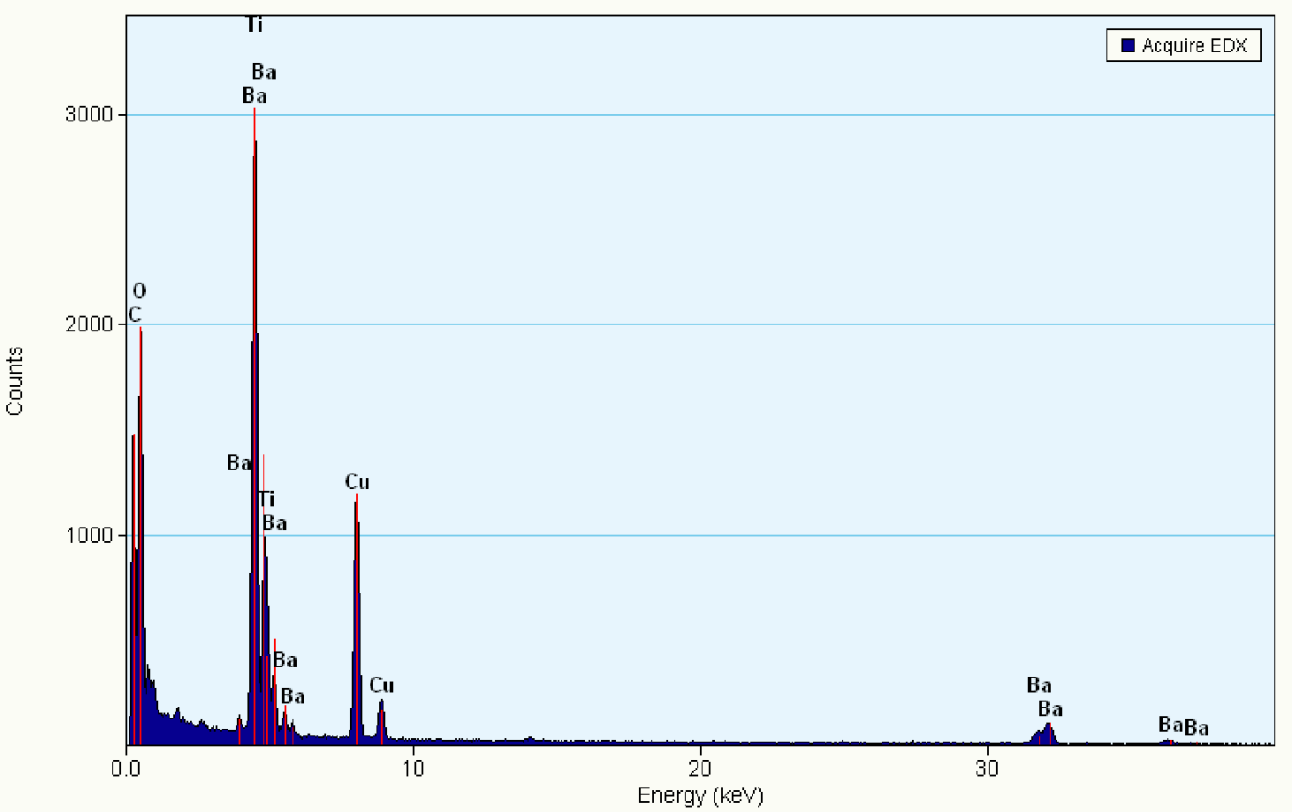

Figure 4.7 Elemental composition graph of EDX integrated into the TEM system

Electron images are so comprehensive that we can use them to visualise particles of micro and nano scale very clearly. One such application is the comparision of nano-BT 100 hour milled particles and bulk BT crystals as shown in Figure 4.8. It is easy to observe that the unmilled BT is in bulk size of about 300-400 nm and shaped as common crystals whereas nano-BT particles(BT100) are nearly spherical in shape with diameters in the range of 15-25 nm. The HRTEM image also shows the grain boundary between nano-BT and the absorbed CO_2 in its mass and the lattice fringes which are evenly spaced showing the interplanar distances for calculating the miller indices of crystal structure and determination of its crystal phase.

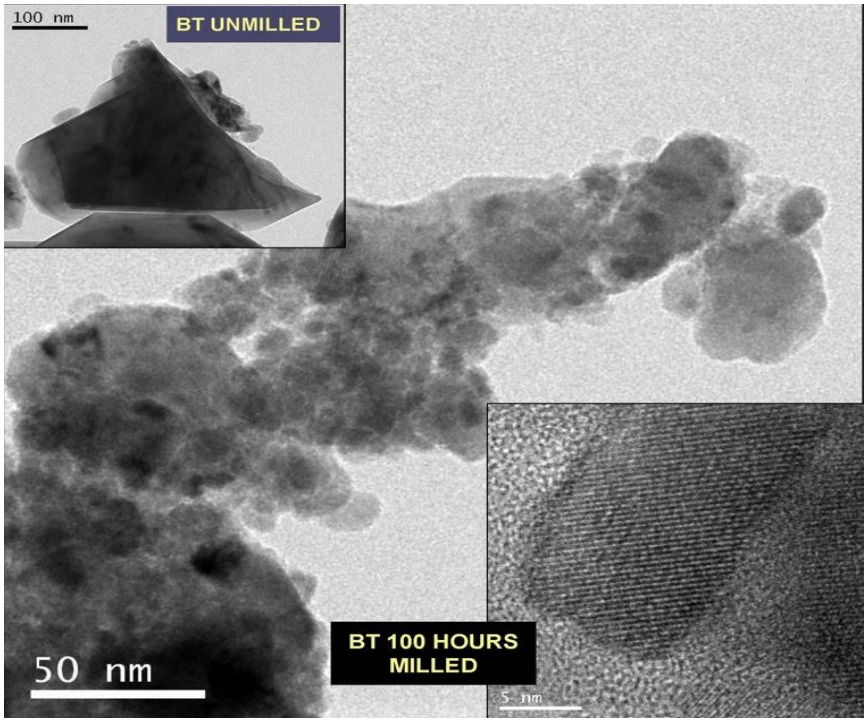

Figure 4.8 Comparision of bulk BT (unmilled) with its nanoparticles(BT100)

4.3. Impedance spectrometry and sensing characteristics

Pellets of nano-BT were formed as desribed in section 3.1.Their dimensions were measured using vernier calipper. Pellet diameter is approximately 10 mm, equal to that of the mould used. Their average thickness is provided in Table 4.3.

Pellet	BT0	BT25	BT50	BT100
Thickness (in mm)	2.45	1.43	1.95	1.92

Table 4.3 Dimensions of pellets made from BT powder milled upto 25 hours (BT25), 50 hours (BT50) and 100 hours (BT100); at 0 hours (BT0), the commercially available BT is unmilled, in its original form.

Periodic measurements of electrical parameters of Barium Titanate nanoparticles, from the first day upto many days after milling, under AC bias at normal atmospheric condition are shown graphically in figures 4.9 and 4.10. Measurements of capacitance (in pF) by varying the frequency under 1 volt AC supply for BT milled upto 25 hours (BT25), 50 hours (BT50) and 100 hours (BT100), are shown graphically in figure 4.9. It denotes a gradual shift in graphs with the repeatition of measurements on regular intervals. At lower frequencies, around 100 Hz, capacitance changes are observed the highest overall, and upto the second day in partucular, for Barium Titanate powders milled upto 100 hours. It can be observed that highest values of capacitance under the

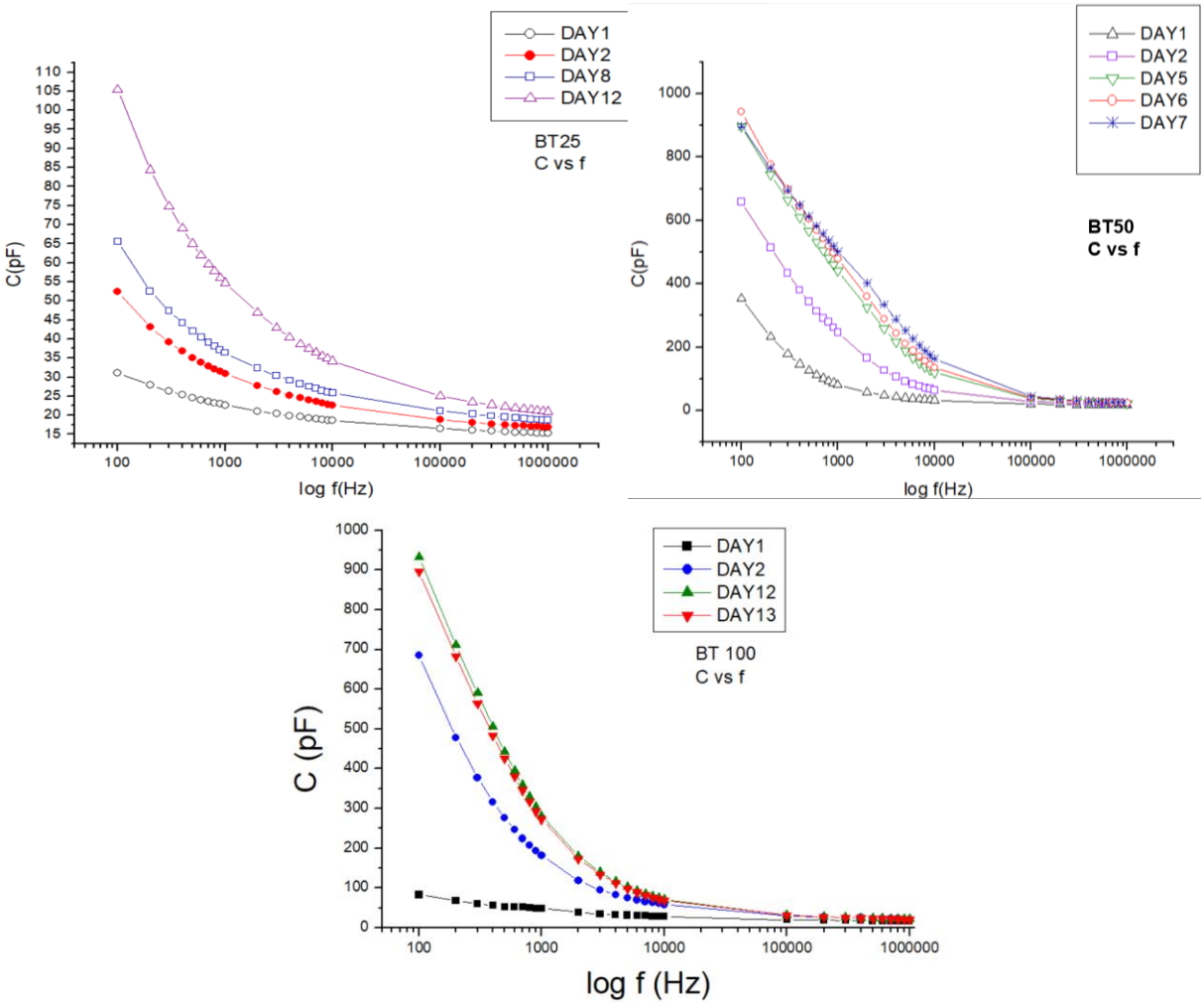

Figure 4.9 Variation of capacitance with frequency for 25, 50 and 100 hours milled BT

same frequency range, varies between 30 pF and 90 pF for BT25, and the same varies between 300 pF to 1000 pF for BT50, inceasing from the first day to the twelfth day measurements in both. It can also be observed that its capacitance increases with the

absorption of CO_2 in the sample over many days, in both of the nanoparticle sizes. This in conformity with the earlier work of Ghosh et al [42]. The particles, about 20 nm in size, show decreament in the rate of change in capacitance thereafter, upto the 10-12 days. Then the capacitance attains almost a saturation value and a little further change is observed. This indicates that CO_2 absorption rate slows down in the material and the absorption seizes after attaining a saturation value.

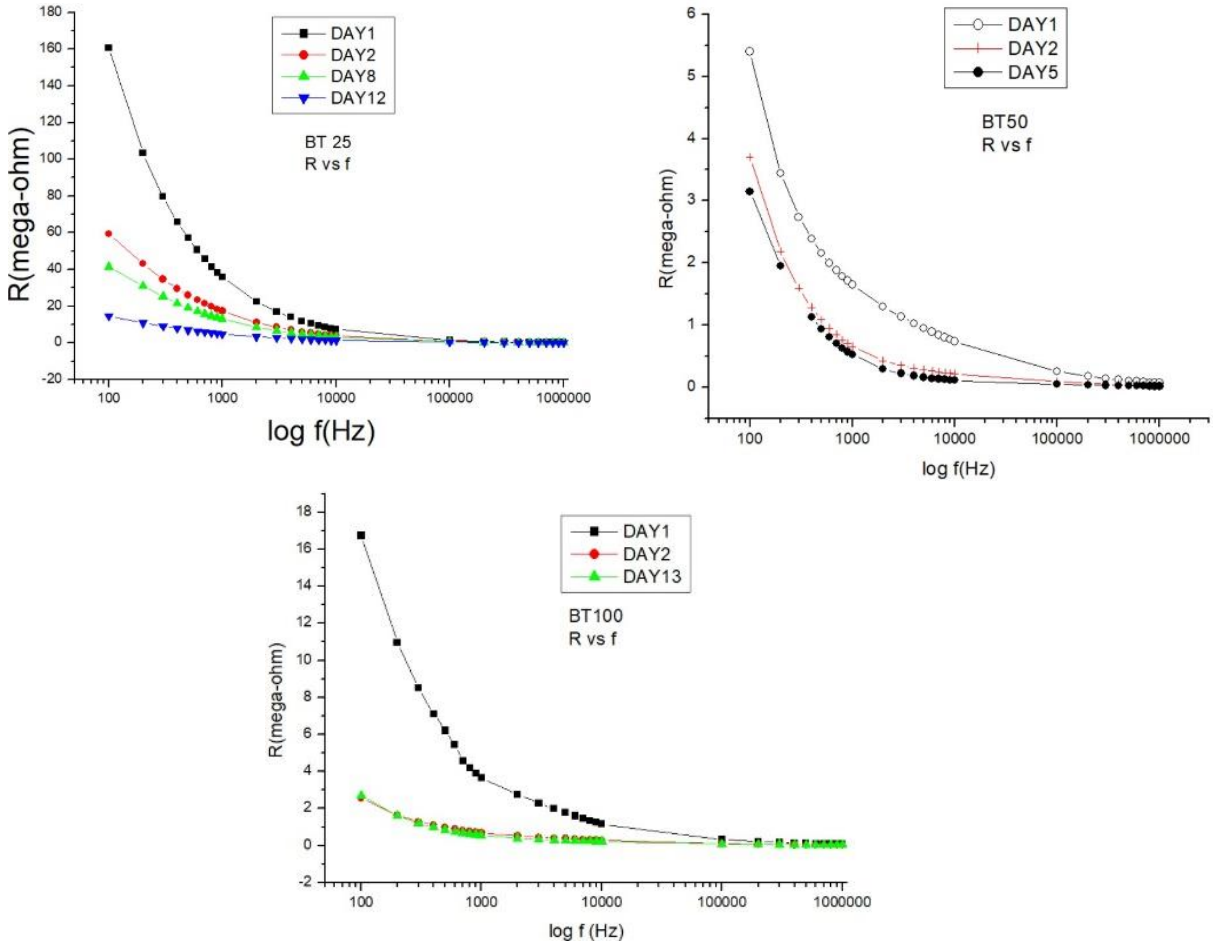

Figure 4.10 Variation of resistance with frequency for 25, 50 and 100 hours milled BT

Figure 4.10 shows the semilog graphs for resistance (in MΩ) plotted against frequency (in hertz) under 1 volt AC supply for BT milled upto 25 hours (BT25), 50 hours (BT50) and 100 hours (BT100). It indicates a gradual shift in graphs with the repetition of measurements at regular intervals. At lower frequencies, around 100 Hz, drastic changes in these parameters are observed, particularly within the period of first two days after their milling. The particle size decreases with increament in milling hours. Hence, BT100 has smaller particles than BT25. A similar variation in its resistance is observed but in the reverse order. This implies that its resistivity decreases with absorption of CO_2 in the BT nanoparticles.

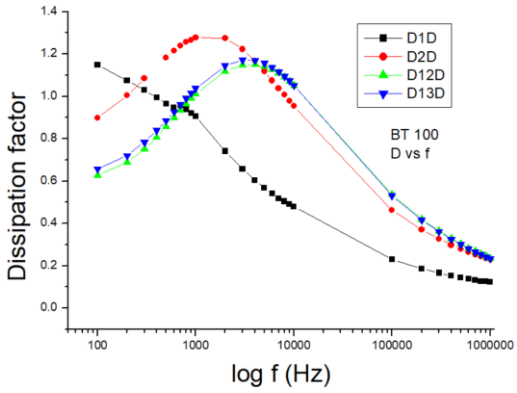

Figure 4.11 Variation of dissipation factor with frequency for 100 hours milled BT

Similar observations can be drawn from the data shown in figure 4.11 for 100 hours milled BT nanoparticles under the similar conditions. It can be observed again, that its electrical parameters vary with absorption of CO_2 over many days. Resistivity decreases over

many days while capacitance increases in the same period. The graph for dissipation factor (D) shows that nano-BT has low value of D at lower frequencies, which increases making a maxima and then decreases almost linearly at higher frequencies to its lowest values. This maxima and the whole graph shifts to the right with absorption of CO_2 over many days. Hence, D of nano-BT decreases at lower frequencies and increases at higher frequencies, with the absorption of CO_2.

Below are some experimental data(table 4.4-4.7) obtained by measurement of electrical parameters of pellets prepared from mechanically milled Barium Titanate nanoparticles, under various biases and conditions.

f (in Hz)	C (in pF) DAY1	C (in pF) DAY2	C (in pF) DAY12	C (in pF) DAY13
100	82.7824	685.411	932.682	895.465
200	67.5903	478.639	710.915	682.252
300	60.581	376.862	590.423	564.119
400	56.25	316.651	506.34	483.52
500	53.1103	275.761	443.288	425.471
600	51.3881	246.28	395.323	381.197
700	51.8445	224.101	358.794	345.749
800	50.4031	206.555	329.038	316.861
900	49.168	193.27	303.088	292.943
1000	48.1346	181.207	281.079	272.916
2000	38.8465	118.293	180.5	173.398
3000	35.1553	95.4143	139.465	134.243
4000	32.9076	83.2179	117.311	112.627
5000	31.567	75.4628	102.959	98.5355
6000	30.5296	69.9969	93.0548	89.0146
7000	29.9051	66.0032	85.4431	81.8608
8000	29.286	62.7534	79.5667	76.3935
9000	28.7966	60.3123	74.6836	71.9633
10000	28.5184	58.1982	70.6915	68.2513
100000	20.3128	30.8306	32.1101	31.504
200000	18.9531	27.1205	27.7635	27.2843
300000	18.3523	25.4182	25.7187	25.3847
400000	17.977	24.3757	24.4864	24.2374
500000	17.7129	23.672	23.6441	23.425
600000	17.5137	23.1347	23.0426	22.833
700000	17.365	22.6988	22.5525	22.3533
800000	17.2618	22.3571	22.1449	21.9675
900000	17.2452	22.057	21.8129	21.6414
1000000	17.1607	21.8116	21.5079	21.3615

Table 4.4 Capacitace values recorded over multiple days for 100 hour milled nano-BT pellet(BT100) under 1 volt AC supply and varying frequency.

The data reveals the capacitance values (in pF) of nanobarium titanate at different frequencies, providing valuable insights into its CO_2 absorption capabilities. Analyzing the data reveals some interesting trends. Firstly, there appears to be an inverse relationship between frequency and capacitance. As the frequency increases, the capacitance values generally decrease. Furthermore, the data shows gradual variation in

capacitance values over subsequent days. At lower frequencies (100-1000 Hz), the capacitance values were relatively high, ranging from 48.13 pF to 932.68 pF, demonstrating the efficient CO_2 sensing capabilities of the BT pellet(table 4.4). As the frequency increased, the capacitance values decreased gradually, indicating a reduced sensitivity to CO_2. This suggest that the CO_2 sensing characteristics of the BT pellets are more pronounced at lower frequencies, indicating a higher sensitivity to CO_2 in this frequency range.

f (in Hz)	C (in pF) DAY1	C (in pF) DAY2	C (in pF) DAY5	C (in pF) DAY6	C (in pF) DAY7
100	352.849	658.017	897.614	942.484	896.633
200	232.201	514.206	745.966	777.187	765.19
300	177.632	434.061	664.54	698.218	695.273
400	145.497	380.383	609.245	644.612	648.159
500	125.195	342.756	567.645	603.323	612.053
600	111.204	313.66	532.714	569.965	582.684
700	100.641	290.347	506.296	542.56	557.998
800	92.5392	278.779	481.612	518.345	536.678
900	86.0877	261.639	460.294	497.641	518.082
1000	80.9971	246.844	441.487	479.078	501.481
2000	56.7051	165.172	325.975	359.608	401.884
3000	47.6989	126.598	258.288	289.026	333.961
4000	42.8722	105.517	215.96	243.331	287.355
5000	39.692	92.2178	187.1	211.502	253.013
6000	37.4698	83.0293	166.167	187.868	226.677
7000	35.7339	76.5586	150.196	169.654	205.629
8000	34.2965	71.3645	137.803	155.783	188.699
9000	33.2004	67.4946	127.774	144.192	174.763
10000	32.292	64.2498	119.54	134.616	163.051
100000	20.4834	29.0528	38.1596	40.1804	43.988
200000	18.72	25.1517	31.3408	32.5945	34.8589
300000	17.8923	23.3548	28.4166	29.4424	31.1738
400000	17.4023	22.2914	26.7302	27.6121	29.061
500000	17.0604	21.5739	25.5858	26.3874	27.643
600000	16.8148	21.0369	24.7547	25.4901	26.6067
700000	16.6149	20.6259	24.1206	24.7852	25.8265
800000	16.4434	20.2872	23.5986	24.2345	25.1796
900000	16.3107	20.0059	23.1704	23.7791	24.6515
1000000	16.1885	19.7886	22.8141	23.3883	24.228

Table 4.5 Capacitace values recorded over multiple days for 50 hour milled nano-BT pellet(BT50) under 1 volt AC supply and varying frequency.

The capacitance values for the 50-hour milled powder are generally lower than those of the 100-hour milled powder at the same frequencies(table 4.5). This indicates that the 50-hour milled nano-BT powders have a comparatively lower CO_2 absorption capacity. The capacitance values for the 50-hour milled powder increase to a lesser extent as the number of days increases, suggesting a slower CO_2 absorption rate. Similar to the 100-hour milled powder, the capacitance values of the 50-hour milled powder decrease as the frequency increases. However, the magnitude of the decrease is higher for the 50-hour milled powder, indicating that it is less responsive to CO_2 at higher frequencies.

The 50-hour milled powder shows a gradual increase in capacitance values over time, whereas the 100-hour milled powder exhibited a more significant increase. This implies that the 50-hour milled powder reaches its CO_2 absorption saturation point sooner compared to the 100-hour milled powder. The 100-hour milled powder demonstrated a more efficient CO_2 sensing behavior overall, with higher capacitance values and a larger range of change. The 50-hour milled powder, although capable of CO_2 sensing, appears to have lower overall efficiency and sensitivity. Thus, The 100-hour milled powder exhibited higher capacitance values, greater sensitivity to CO_2, and a more pronounced response over time. In contrast, the 50-hour milled powder showed lower capacitance values, reduced sensitivity, and a slower response. The comparison between the 100-hour and 50-hour milled nano-BT powders indicates that the milling duration significantly affects the CO_2 sensing behavior.

f (in Hz)	C (in pF) DAY1	C (in pF) DAY2	C (in pF) DAY8	C (in pF) DAY12
100	31.0656	52.4789	65.5089	105.329
200	27.8995	43.0798	52.5799	84.391
300	26.2977	39.1309	47.3802	74.8392
400	25.3041	36.7592	44.2049	69.0082
500	24.5723	35.127	42.053	64.9825
600	24.0123	33.8622	40.4751	61.9595
700	23.6041	32.8934	39.1607	59.6121
800	23.2663	32.1149	38.0962	57.705
900	22.9547	31.4714	37.1951	56.0904
1000	22.6655	30.8694	36.4029	54.7201
2000	21.0922	27.7669	32.3377	46.9609
3000	20.3375	26.227	30.3331	42.9007
4000	19.8595	25.2487	29.124	40.4321
5000	19.5214	24.5216	28.2077	38.6714
6000	19.2477	23.9807	27.5337	37.3905
7000	19.0376	23.5566	27.0091	36.3991
8000	18.8722	23.1944	26.4977	35.4954
9000	18.7166	22.8726	26.1123	34.8145
10000	18.6067	22.5986	25.7479	34.2033
100000	16.4909	18.8482	21.147	25.0594
200000	16.0362	18.1131	20.2719	23.4898
300000	15.8251	17.749	19.81	22.7249
400000	15.6575	17.5042	19.5097	22.2414
500000	15.5629	17.3183	19.2868	21.8855
600000	15.4793	17.1709	19.1217	21.6167
700000	15.4033	17.0586	18.9718	21.406
800000	15.3418	16.9536	18.8458	21.2276
900000	15.2862	16.8694	18.7559	21.0726
1000000	15.2473	16.7978	18.6752	20.9448

Table 4.6 Capacitace values recorded over multiple days for 25 hour milled nano-BT pellet(BT25) under 1 volt AC supply and varying frequency.

The capacitance values for the 25-hour milled pellets are further lower than those of the 50 and100-hour milled pellets at the same frequencies(table 4.6). This suggests that the 25-hour milled BT pellets also have a lower CO_2 absorption capacity. The capacitance values for the 25-hour milled pellets increase to a lesser extent as the number of days increases, indicating a slower CO_2 absorption rate. The 25-hour milled pellets show a

gradual increase in capacitance values over time, but the magnitude of the increase is smaller compared to the 50 and 100-hour milled pellets. This implies that the 25-hour milled pellets reach their CO_2 absorption saturation point sooner compared to the 50 and 100-hour milled pellets.The 25-hour milled pellets showed lower capacitance values, reduced sensitivity, and a slower response.The comparison between the 25, 50 and 100-hour milled BT pellets also indicates that the milling duration significantly affects the CO_2 sensing behavior. Again, this suggests that longer milling durations enhance the CO_2 sensing characteristics of BT pellets. It is important to consider the milling duration when optimizing BT pellets for CO_2 sensing applications.

f (in Hz)	C (in pF) DAY1	C (in pF) DAY2	C (in pF) DAY5	C (in pF) DAY6	C (in pF) DAY7	C (in pF) DAY8
100	13.4642	34.6426	44.5862	48.7424	25.2617	35.0777
200	13.2238	26.8363	37.934	39.7153	21.926	30.2435
300	13.0792	24.6564	35.3719	35.5685	20.6421	28.2883
400	13.0273	23.391	34.4627	32.9546	19.8127	27.2207
500	12.988	22.4055	33.4215	30.8565	19.2447	26.4869
600	12.9696	21.6499	32.6072	31.5067	18.799	25.9612
700	12.949	21.0664	32.2895	30.6936	18.4617	25.5899
800	12.9201	20.5416	31.7785	30.0726	18.1446	25.2516
900	12.8942	20.0112	31.3183	29.5828	17.8966	25.1298
1000	12.8898	19.5975	30.9664	29.1179	17.6892	25.0194
2000	12.6875	18.2134	27.8856	26.0002	16.7292	22.9018
3000	12.5817	17.5015	26.306	24.5051	16.2595	21.9552
4000	12.5473	16.9119	25.3707	23.6162	15.9589	21.3824
5000	12.4759	16.594	24.7188	22.9857	15.751	20.954
6000	12.4198	16.2907	24.3182	22.4751	15.6149	20.6917
7000	12.3711	16.0251	23.9467	22.1341	15.4639	20.4827
8000	12.3667	15.8075	23.6458	21.8954	15.3297	20.3377
9000	12.3582	15.5648	23.4007	21.6423	15.197	20.247
10000	12.3396	15.3944	23.159	21.4274	15.1107	20.1814
100000	11.6473	13.7535	18.7615	17.5756	13.8003	16.9796
200000	11.4244	13.3293	17.9086	16.7969	13.4566	16.325
300000	11.3165	13.0572	17.4493	16.3944	13.2468	15.9491
400000	11.2235	12.8119	17.1671	16.1349	13.0812	15.6942
500000	11.1405	12.67	16.9392	15.942	12.9495	15.4231
600000	11.0899	12.5376	16.7917	15.7791	12.8429	15.2097
700000	11.0429	12.4443	16.6642	15.6596	12.7608	15.0295
800000	11.0048	12.3357	16.5421	15.5494	12.6753	14.8333
900000	10.9678	12.256	16.4564	15.4628	12.6043	14.7005
1000000	10.9352	12.1775	16.3639	15.3939	12.5423	14.5649

Table 4.7 Capacitace values recorded over multiple days for unmilled BT pellet(BT0) under 1 volt AC supply and varying frequency.

The capacitance values of the unmilled BT bulk particles are significantly lower than those of the ball-milled nano-BT powder across all frequencies and time periods (table 4.7). The milled BT powders exhibited higher capacitance values, indicating a greater CO_2 sensing capability. The unmilled BT bulk particles did not exhibit significant changes in capacitance, indicating their lack of CO_2 absorption or sensing behavior.

Both the unmilled BT bulk particles and the ball-milled nano-BT powder exhibited a decrease in capacitance values with increasing frequency. However, the capacitance values of the milled nano-BT powder were consistently higher than those of the unmilled bulk particles at each frequency, emphasizing its superior CO_2 sensing potential.

Thus, the comparison between the unmilled BT bulk particles and the ball- milled nano-BT powder highlights the importance of the milling process in enhancing the CO_2 sensing behavior of BT nanoparticles. The ball-milled nano-BT powder demonstrated higher capacitance values and a responsive CO_2 sensing behavior, while the unmilled bulk particles showed minimal capacitance changes and lacked CO_2 absorption capacity.

Effect of particle size reduction in BT by mechanical milling on the absorption of CO_2 by nano-BT, has been demonstrated through these results. Electrical measurements recorded on samples of nano-BT obtained at various milling hours provides adequate selectivity for developing a CO_2 sensor by optimising sensitivity and response time. The room temperature measurements successfully indicate a gradation in properties such as resistivity and capacitance with the applied frequency, by repeated measurements at regular intervals over a period of many days.

The performance of nanoscale materials and devices is heavily influenced by temperature variations, making temperature-dependent characterization essential for understanding their behavior. Hence, we investigate the V-I (voltage-current) characteristics of nano-BT (Barium Titanate) pellets using temperature-controlled DC measurements. The obtained results shed light on the electrical properties of nano-BT pellets across a range of temperatures, providing valuable insights for its CO_2 sensing behaviour.

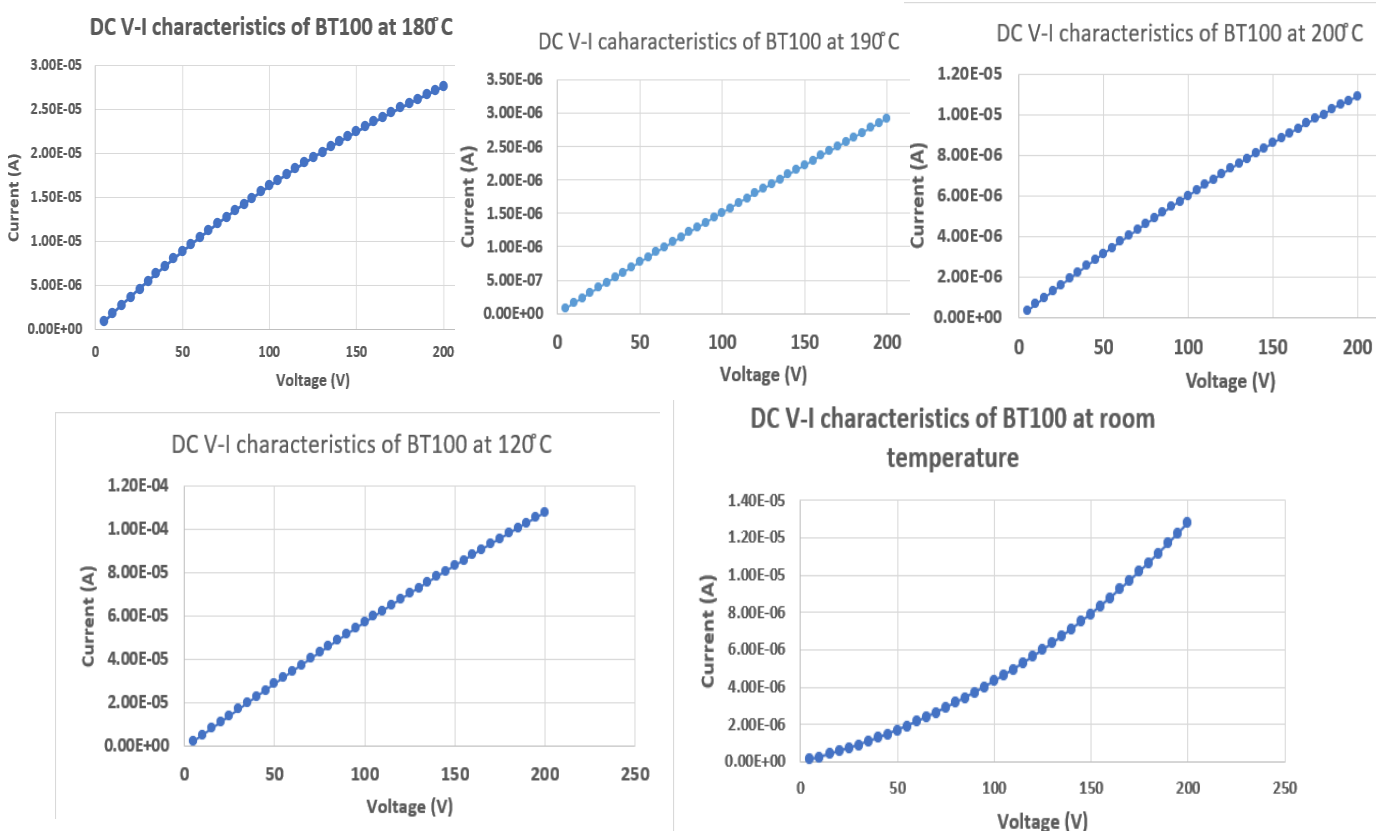

Figure 4.12 V-I characteristics for 100 hour milled nano-BT (BT100) under DC bias.

V-I characteristics obtained by temperature controlled DC measurements for nano-BT pellets(BT100) are shown in figure 4.12. The corresponding data is given in table 4.8. Overall, a linear V-I characteristics has been obtained at different temperature ranges between room temperature to 200 ºC. At any particular temeperature, the current is found to be proportional to voltage in the range of 5 volt to 200 volt. But current

Voltage (in volt)	Current (in ampere at RT*)	Current (in ampere at 120℃)	Current (in ampere at 180℃)	Current (in ampere at190℃)	Current (in ampere at 200℃)
5	1.12E-07	2.14E-06	9.11E-07	7.60E-08	3.13E-07
10	2.44E-07	5.03E-06	1.87E-06	1.54E-07	6.40E-07
15	3.95E-07	7.94E-06	2.80E-06	2.32E-07	9.63E-07
20	5.53E-07	1.09E-05	3.71E-06	3.09E-07	1.28E-06
25	7.20E-07	1.39E-05	4.62E-06	3.87E-07	1.60E-06
30	8.93E-07	1.68E-05	5.51E-06	4.64E-07	1.91E-06
35	1.08E-06	1.98E-05	6.38E-06	5.40E-07	2.22E-06
40	1.27E-06	2.28E-05	7.23E-06	6.17E-07	2.53E-06
45	1.47E-06	2.57E-05	8.07E-06	6.93E-07	2.84E-06
50	1.68E-06	2.87E-05	8.90E-06	7.68E-07	3.14E-06
55	1.90E-06	3.16E-05	9.71E-06	8.44E-07	3.44E-06
60	2.14E-06	3.45E-05	1.05E-05	9.19E-07	3.73E-06
65	2.37E-06	3.74E-05	1.13E-05	9.94E-07	4.03E-06
70	2.63E-06	4.03E-05	1.20E-05	1.07E-06	4.32E-06
75	2.88E-06	4.31E-05	1.28E-05	1.14E-06	4.61E-06
80	3.15E-06	4.59E-05	1.35E-05	1.22E-06	4.89E-06
85	3.42E-06	4.87E-05	1.43E-05	1.29E-06	5.17E-06
90	3.70E-06	5.15E-05	1.50E-05	1.36E-06	5.45E-06
95	4.00E-06	5.43E-05	1.57E-05	1.44E-06	5.73E-06
100	4.30E-06	5.70E-05	1.64E-05	1.51E-06	6.00E-06
105	4.62E-06	5.97E-05	1.70E-05	1.58E-06	6.28E-06
110	4.94E-06	6.24E-05	1.77E-05	1.66E-06	6.54E-06
115	5.27E-06	6.51E-05	1.83E-05	1.73E-06	6.81E-06
120	5.62E-06	6.78E-05	1.90E-05	1.80E-06	7.08E-06
125	5.97E-06	7.04E-05	1.96E-05	1.87E-06	7.34E-06
130	6.33E-06	7.30E-05	2.02E-05	1.94E-06	7.59E-06
135	6.71E-06	7.56E-05	2.08E-05	2.01E-06	7.85E-06
140	7.10E-06	7.82E-05	2.14E-05	2.08E-06	8.10E-06
145	7.50E-06	8.07E-05	2.20E-05	2.15E-06	8.35E-06
150	7.91E-06	8.32E-05	2.25E-05	2.22E-06	8.60E-06
155	8.33E-06	8.58E-05	2.31E-05	2.29E-06	8.85E-06
160	8.78E-06	8.83E-05	2.36E-05	2.37E-06	9.09E-06
165	9.23E-06	9.08E-05	2.42E-05	2.43E-06	9.33E-06
170	9.69E-06	9.32E-05	2.47E-05	2.50E-06	9.57E-06
175	1.02E-05	9.57E-05	2.52E-05	2.57E-06	9.80E-06
180	1.07E-05	9.81E-05	2.57E-05	2.64E-06	1.00E-05
185	1.12E-05	1.01E-04	2.62E-05	2.71E-06	1.03E-05
190	1.17E-05	1.03E-04	2.67E-05	2.78E-06	1.05E-05
195	1.22E-05	1.05E-04	2.72E-05	2.85E-06	1.07E-05
200	1.28E-05	1.08E-04	2.77E-05	2.92E-06	1.09E-05

Table 4.8 Values of electric current through BT100 pellet under dc voltages at different temperatures(*RT=Room Temperature).

magnitude through the nano-BT pellet is dependent on the temperature applied to it. The current magnitude was found to be the highest at 120 ºC in the range of hundreds of milliamperes. The current was in the microampere range around lower and higher temperatures. The provided data allows us to analyze the V-I characteristics of the nano-BT pellets obtained at different temperatures(table 4.8). The current values at room temperature, 120°C, 180°C, 190°C, and 200°C for various applied voltages are given. At all temperatures, the relationship between voltage and current follows an ohmic behavior, as indicated by the linear V-I characteristics. This implies that the current passing through the nano-BT pellet is directly proportional to the applied voltage within the given voltage range.

At room temperature, the current values range from approximately 1.12E-07 A at 5 V to 1.28E-05 A at 200 V. As the temperature increases to 120°C, the current magnitude

rises significantly, reaching values between 2.14E-06 A and 5.70E-05 A. This trend suggests enhanced conductivity and higher charge carrier mobility at elevated temperatures. However, as the temperature continues to increase to 180°C, 190°C, and 200°C, the current magnitude begins to decrease. The current values range from 2.77E-05 A to 2.92E-06 A at 200 V, indicating a decrease in charge carrier mobility and conductivity at these higher temperatures.

It is worth noting that the highest current magnitude is observed at 120°C, where the nano-BT pellet exhibits current values in the range of hundreds of microamperes. This temperature range appears to optimize the charge transport properties within the nano-BT material, resulting in significantly enhanced conductivity. Conversely, at lower and higher temperatures, the current magnitude decreases, falling into the microampere range. This behavior suggests reduced charge carrier mobility and conductivity outside the optimal temperature range of 120°C. The temperature dependence of the current magnitude highlights the importance of considering the operating temperature when utilizing nano-BT pellets in electronic devices or sensors. The findings from this study provide valuable insights for optimizing the performance of nano-BT-based applications that rely on specific temperature ranges.

Thus, the V-I characteristics of the nano-BT pellet(BT100) exhibits a linear relationship between voltage and current within the applied voltage range. The current magnitude is highly dependent on temperature, with the highest values observed in the range of 120°C. This temperature-induced variation in current magnitude underscores the significance of temperature control and optimization in harnessing the electrical properties of nano-BT pellets for CO_2 sensing and other applications.

After measurement of the resulting changes in resistance or capacitance while exposed to different concentrations of CO_2 gas, calibration curves are needed to establish a relationship between the measured values to the standard values of reference samples. The calibration curve is obtained using following steps:

- Reference standards are gathered.
- The response or signal for each of the reference standards is measured.
- The calibration curve is plotted by the measured response values on the y-axis against the corresponding known values on the x-axis.
- A mathematical function or equation is fitted to the calibration curve.
- The calibration curve is evaluated to assess its goodness of fit.

The calibration curve is used to determine the unknown values of samples based on their measured responses by comparing the measured response of an unknown sample to the calibration curve for estimating the corresponding unknown value.

Standard reference samples have been created in this study by mixing known concentrations of commercially available Barium Carbonate(BC) powder to 100 hour milled nano-BT powder to form standard pellets containing 2.5%, 5%, 7.5%, and 10% w/w of BC. Standard pellet details are summarised in table 4.9 below.

Std. reference sample	BT1002.5	BT1005	BT1007.5	BT10010
Nano-BT Wt. (in g)	0.5	0.5	0.5	0.5
BC Wt. (in g)	0.0125	0.025	0.0375	0.05
BC (w/w %)	2.5	5	7.5	10
CO2 (w/w %)	0.150	0.301	0.452	0.602

Table 4.9 Composition of standard reference samples of nano-BT.

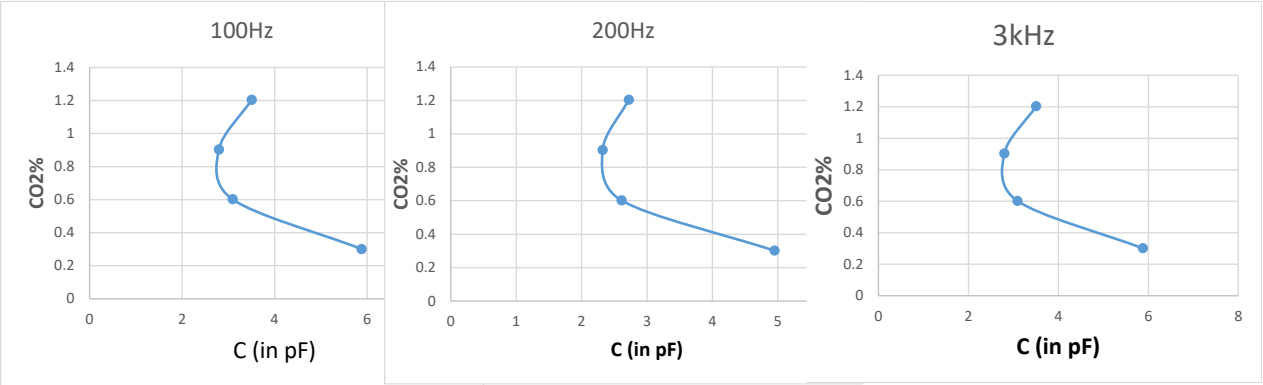

Figure 4.13 Capacitance variation with CO2 concentration in nano-BT (BT100) standard reference samples.

The curves obtained for standard reference samples, showing the relation of carbon dioxide concentration in the nano-BT pellets with their capacitance values (figure 4.13) clearly demonstrate a future scope for development of CO2 sensor using nanocrystalline BT.

Chapter 5
Use of nano-BT as a gas sensor

Nano-BT (nanostructured barium titanate) is a promising material that has gained significant attention for its potential use as a gas sensor. It exhibits high surface area and enhanced reactivity due to its nanoscale structure. This characteristic enables a higher probability of gas molecules interacting with the material's surface, leading to improved sensitivity and response. The large surface-to-volume ratio of nano-BT allows for efficient gas adsorption and desorption processes, facilitating rapid and accurate detection of target gases[35-40].

One of the gas sensing mechanism of nano-BT is based on the changes in its electrical properties upon exposure to specific gases. In our study, CO_2 gas readily absorbed by these nanoparticles leads to gradual changes in electrical parameters of the material. When gas molecules interact with the surface of nano-BT, they can donate or accept electrons, altering the conductivity or dielectric properties of the material. This change in electrical properties has been measured and summarised in the previous chapter. This can be correlated to the concentration of the target gas.

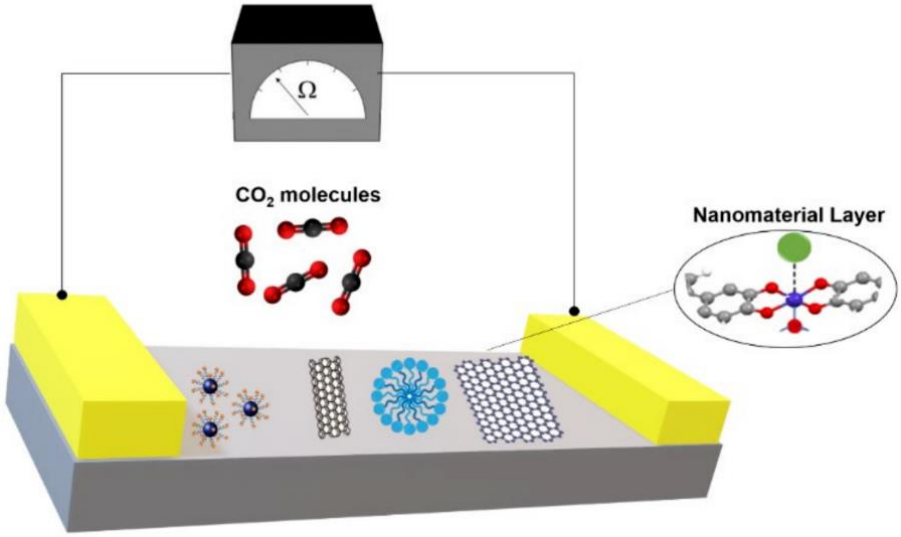

Figure 5.1 Schematic diagram for sensing mechanism of CO_2 sensors using nanomaterials; ; modified from [33].

5.1. Various possibilities for developing CO_2 sensors

The ability of nano-BT to undergo changes in its electrical properties upon exposure to CO_2 makes it a suitable candidate for CO_2 sensing applications. There are several possibilities for developing sensors specifically for carbon dioxide (CO_2) detection[33]:

Resistive Sensor: A resistive sensor based on nano-BT can be developed for CO_2 detection. The absorption of CO_2 gas by the nanoparticles will result in changes in the resistance of the material. By measuring the resistance, the concentration of CO2 can be determined.

Capacitive Sensor: Another approach is to develop a capacitive sensor using nano-BT. The absorption of CO_2 by the nanoparticles will alter the dielectric properties of the

material, leading to changes in capacitance. By measuring the capacitance, the presence and concentration of CO_2 can be detected.

Optical Sensor: Nano-BT can also be utilized in the development of optical CO_2 sensors. The changes in electrical properties induced by CO_2 absorption can affect the material's optical properties, such as refractive index or absorption spectrum. By monitoring these optical changes, the presence and concentration of CO_2 can be determined.

Field-Effect Transistor (FET) Sensor: Nano-BT can be incorporated into a FET-based sensor configuration. The absorption of CO_2 gas will modulate the conductivity or threshold voltage of the FET, allowing for the detection and quantification of CO_2.

In all of these sensor configurations, the gradual changes in electrical parameters of the nano-BT material caused by the absorption of CO2 gas enable the detection and quantification of CO_2 concentrations. By carefully designing the sensor structure and optimizing the nano-BT properties, highly sensitive and selective CO_2 sensors can be developed for environmental monitoring, indoor air quality control, and other CO_2-related applications.

5.2. Implementation of nano-BT in optoelectronic sensors

Nano-BT can be employed in the construction of an optical sensor for CO_2 detection by utilizing its ability to induce changes in the material's optical properties upon CO_2 absorption. When CO_2 gas interacts with the nanostructured surface of the material, it can lead to alterations in the material's refractive index or absorption spectrum, providing a basis for CO_2 sensing.

In this type of sensor, light is typically passed through or reflected off the nano-BT material, and the resulting optical changes are measured and analyzed to determine the presence and concentration of CO_2. Several optical sensing techniques can be utilized:

Interferometric Techniques: Interferometric techniques, such as Fabry-Perot interferometry or Mach-Zehnder interferometry, can be employed[41]. In these setups, the interference patterns of light passing through or reflecting off the nano-BT material are analyzed. CO_2 absorption-induced changes in the material's refractive index lead to alterations in the interference patterns, enabling CO_2 detection.

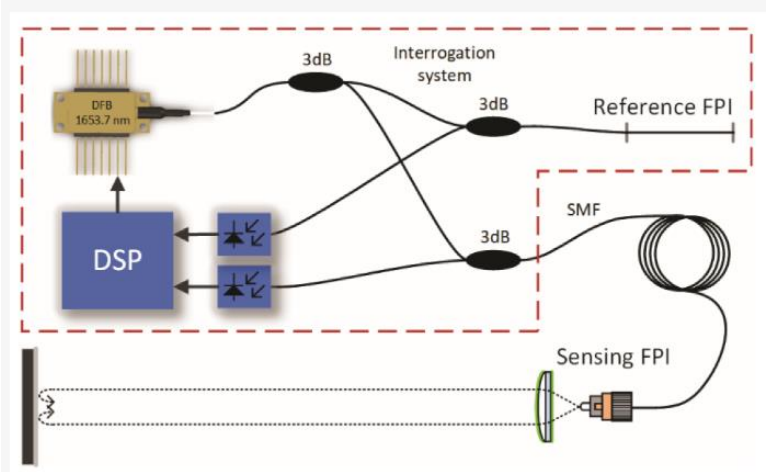

Figure 5.2 Basic system setup of Fabry-Perot gas sensing interferometer[41].

Absorption Spectroscopy: By employing absorption spectroscopy, the sensor can detect changes in the absorption spectrum of nano-BT caused by CO_2 absorption. The presence of CO_2 alters the absorption characteristics of the material, leading to shifts or changes in the intensity of specific wavelengths of light. This shift can be measured and correlated to the concentration of CO_2 in the environment.

Reflectance Spectroscopy: In reflectance spectroscopy, the nano-BT material is illuminated with light, and the reflected light is analyzed. The presence of CO_2 alters the refractive index of the material, causing changes in the reflected light's intensity or wavelength. These changes can be detected and used to determine the concentration of CO_2.

Specifically, laser technology offers several possibilities for CO_2 sensing using nano-BT material:

Laser Absorption Spectroscopy: Laser absorption spectroscopy can be employed to detect and quantify CO_2 concentrations using nano-BT. A laser source emitting at a specific wavelength, typically within the infrared range where CO_2 absorption bands occur, can be directed through the nano-BT material. As CO_2 molecules absorb the laser light, the intensity of the transmitted or reflected light changes. By measuring the intensity variation, the CO_2 concentration can be determined.

Tunable Laser Sources: Tunable lasers can provide flexibility in choosing the optimal wavelength for CO_2 sensing with nano-BT. These lasers can be adjusted to emit light at specific wavelengths corresponding to the absorption bands of CO_2. This enables precise targeting of the absorption features of CO_2 and enhances the sensitivity and selectivity of the sensor.

Laser-Induced Fluorescence: Laser-induced fluorescence (LIF) techniques can be utilized for CO_2 sensing with nano-BT. By irradiating the nano-BT material with a laser at an appropriate excitation wavelength, the absorbed energy can induce fluorescence emission. The fluorescence intensity can be measured, and changes in the emitted light can indicate the presence and concentration of CO_2.

Raman Spectroscopy: Raman spectroscopy, combined with laser excitation, can be utilized for CO_2 sensing with nano-BT. When a laser beam interacts with the nano-BT material, it induces Raman scattering, resulting in a characteristic spectrum. By analyzing the shifts and intensities of the Raman peaks, CO_2 concentrations can be determined.

Laser Interferometry: Laser interferometry techniques can be employed to measure changes in the refractive index or optical path length of the nano-BT material induced by CO_2 absorption. Interference patterns produced by laser beams passing through the material can be analyzed to determine CO_2 concentrations. This approach offers high sensitivity and accuracy in CO_2 sensing.

Additionally, fiber optics can be implemented in CO_2 sensing with nano-BT. This involves several steps and considerations:

Selection of Fiber Optic Type: The appropriate fiber optic cable for the sensing application is chosen. Single-mode or multi-mode fibers can be used, depending on the

specific requirements such as sensing range, signal stability, and data transmission capacity.

Preparing the Fiber Optic Cable: The fiber optic cable is cleaned and prepared to ensure optimal performance. Any contaminants or coatings that may interfere with the interaction between the guided light and the nano-BT material are removed.

Coating the Fiber Optic Cable: The fiber optic cable is coated with a nano-BT coating using techniques such as dip coating, spin coating, or vapor deposition. The coating thickness is carefully controlled to maximize CO_2 absorption and ensure uniform coverage along the fiber.

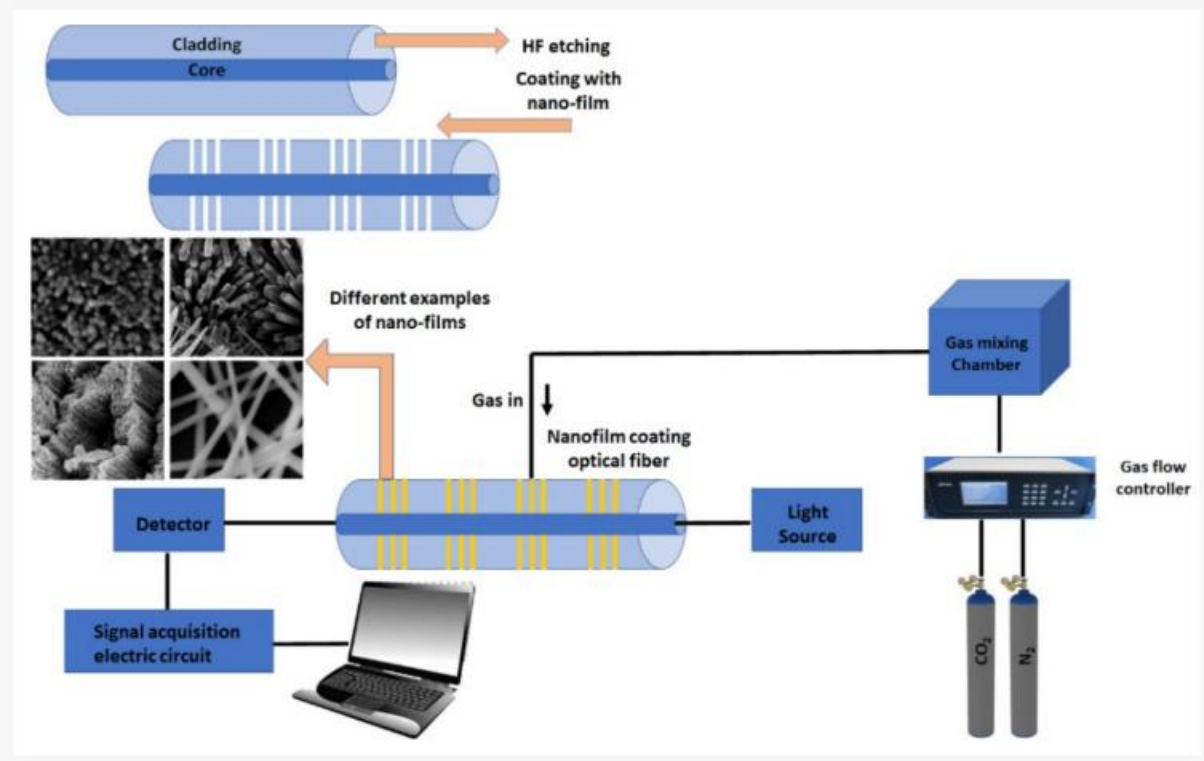

Figure 5.3 The use of nanomaterials thin film in fiber optics based sensors; modified from [33].

Sensor Configuration: The sensing configuration is determined based on the specific CO_2 sensing mechanism. For example, in absorption spectroscopy, the coated fiber can be used as a transmission or reflection-based sensor, where light is transmitted through or reflected off the nano-BT coating.

Light Source and Detection: An appropriate light source, such as an LED or laser diode, and a suitable detection system, such as photodiodes or spectrometers, are selected. The light source emits wavelengths that are sensitive to the changes induced by CO_2 absorption in the nano-BT material.

Signal Conditioning and Analysis: The optical signals obtained from the fiber optic sensor are processed and analyzed. This may involve signal conditioning, such as amplification or filtering, and data analysis techniques to determine the CO_2 concentration based on the measured optical changes.

Calibration and Validation: The sensor is calibrated by exposing it to known CO_2 concentrations to establish a correlation between the measured optical signal and the actual CO_2 levels. The sensor's performance is validated by comparing its readings with reference measurements or established standards.

Integration and Deployment: The fiber optic CO_2 sensor is integrated into the desired application or system. This could involve incorporating it into environmental monitoring networks, industrial control systems, or wearable devices, depending on the specific requirements.
Maintenance and Monitoring: Regular monitoring and maintenance of the fiber optic CO_2 sensor are carried out to ensure its continued accuracy and reliability. Periodic cleaning and recalibration may be necessary to maintain optimal performance over time.

Thus, the integration of fiber optics with nano-BT for CO_2 sensing involves selecting the appropriate fiber optic cable, preparing and coating it with nano-BT material, configuring the sensor, and employing suitable light sources and detection systems. Signal processing and calibration ensure accurate CO_2 measurements, while integration into various applications and regular maintenance support its practical deployment. This approach represents a promising pathway to advance CO_2 sensing technologies, enabling precise and reliable monitoring of carbon dioxide levels across diverse domains.

Conclusion

The present study focused on investigating the carbon dioxide (CO_2) sensing characteristics of nanocrystalline barium titanate ($BaTiO_3$). The significance of utilizing nanostructured $BaTiO_3$ perovskite material was highlighted, emphasizing its unique properties and potential applications in sensing devices. The objective of this research was to explore the feasibility and effectiveness of using nano-$BaTiO_3$ for CO_2 sensing.

In the literature review, various synthesis methods for producing $BaTiO_3$ nanoparticles were examined, considering their impact on the resulting material properties. The properties of $BaTiO_3$ at the nanoscale were discussed, including their size-dependent behavior and enhanced sensing capabilities. Furthermore, the applications of nanostructured materials, particularly in the field of gas sensing, were explored to establish the relevance and potential of nano-$BaTiO_3$ for CO_2 sensing applications.

The experimental details outlined the methodology employed for the synthesis of nano-BT powder, along with the characterization techniques utilized to assess its structural and microstructural properties. Techniques such as FESEM, TEM, and EDX were employed to examine the morphology, crystal structure, and elemental composition of the synthesized material. Impedance spectrometry was employed to evaluate the sensing characteristics of nano-BT and its response to CO_2.

The study demonstrated the potential use of nano-BT as a gas sensor, with a particular focus on CO_2 sensing. Various possibilities for developing CO_2 sensors utilizing nano-BT were discussed, highlighting the gas sensing mechanism based on changes in electrical properties. The implementation of nano-BT in optoelectronic sensors was explored, emphasizing the compatibility and integration of nano-BT with fiber optics and laser technologies.

In conclusion, this research has provided valuable insights into the carbon dioxide sensing characteristics of nanocrystalline barium titanate. The study has demonstrated the potential of nano-BT as a promising material for CO_2 sensing applications. The findings contribute to the understanding of nanostructured materials and their utilization in gas sensing devices. Further research and development in this field are warranted to optimize the performance and practical implementation of nano-BT-based CO_2 sensors.

Future Scope

There are several key areas that can be explored to enhance the understanding and application of nano barium titanate for CO_2 sensing. Firstly, the study can incorporate PDF and Raman analysis techniques to gain deeper insights into the atomic scale local crystal structure, phase composition, and molecular vibrations of the material. This analysis will provide a more comprehensive understanding to tune the nano-BT for possible applications in sensing devices by modifying its local structure.

Secondly, calibration and optimization of the CO_2 sensing system can be further investigated. This includes fine-tuning the sensor's parameters and optimizing its performance for accurate and reliable CO_2 detection. By conducting rigorous calibration experiments under different conditions, the study can refine the sensor's response and ensure its stability and sensitivity over a wide range of CO_2 concentrations and environmental factors.

Furthermore, the future scope of the study involves the development of a sensor prototype. This includes designing a robust and efficient sensor system based on nano barium titanate and packaging it appropriately for practical applications. The prototype should be capable of real-time CO_2 sensing and demonstrate high sensitivity, selectivity, and stability. By successfully developing a functional sensor prototype, the study can pave the way for the practical implementation of nano barium titanate-based CO_2 sensing systems in various industries and environmental monitoring applications.

Finally, investigating the distinct properties of nanocrystalline $BaTiO_3$, has provided valuable insights about the unique material, for its potential applications in various areas, such as laser in-process sensing, laser safety, and optoelectronic devices due to its ferroelectric, piezoelectric, and photorefractive properties.

Publication List

- "Study of Carbon Dioxide Sensing Characteristics of Barium Titanate Perovskite", Avanish Kumar, Siddhartha Bhattacharya, Santanu Sen and Jiten Ghosh, presented in conference **Perovskite Society of India Meet (PSIM)-2023** jointly organized by Perovskite Society of India and **IIT-Roorkee** at IIT-Roorkee during 1st March to 3rd March 2023.

- This study is to be communicated in an SCI journal.

References

[1] Sustainable Development Goals, the United Nations, www.un.org/en/academic-impact/sustainability

[2] Keeling CD. Climate change and carbon dioxide: an introduction. Proc Natl Acad Sci U S A. 1997 Aug 5;94(16):8273-4. doi: 10.1073/pnas.94.16.8273. PMID: 11607732; PMCID: PMC33714.

[3] Du, B, Tandoc, MC, Mack, ML, Siegel, JA. Indoor CO_2 concentrations and cognitive function: A critical review. Indoor Air. 2020; 30: 1067– 1082. https://doi.org/10.1111/ina.12706

[4] Jacobson, T.A., Kler, J.S., Hernke, M.T. et al. Direct human health risks of increased atmospheric carbon dioxide. Nat Sustain 2, 691–701 (2019). https://doi.org/10.1038/s41893-019-0323-1

[5] Knutti, R., Rogelj, J., Sedláček, J. et al. A scientific critique of the two-degree climate change target. Nature Geosci 9, 13–18 (2016). https://doi.org/10.1038/ngeo2595

[6] Scott, V., Gilfillan, S., Markusson, N. et al. Last chance for carbon capture and storage. Nature Clim Change 3, 105–111 (2013). https://doi.org/10.1038/nclimate1695

[7] A. Molina, V. Escobar-Barrios, J. Oliva, A review on hybrid and flexible CO_2 gas sensors, Synthetic Metals, Vol 270, 2020, 116602, ISSN 0379-6779, https://doi.org/10.1016/j.synthmet.2020.116602.

[8] Bhaliya, J.D., Shah, V.R., Patel, G. et al. Recent Advances of MOF-Based Nanoarchitectonics for Chemiresistive Gas Sensors. J Inorg Organomet Polym (2023). https://doi.org/10.1007/s10904-023-02597-w

[9] C. Hao et al., "Greenhouse Gas Detection Based on Infrared Nanophotonic Devices," in IEEE Open Journal of Nanotechnology, vol. 4, pp. 10-22, 2023, doi: 10.1109/OJNANO.2022.3233485.

[10] Marques, G.; Saini, J.; Dutta, M.; Singh, P.K.; Hong, W.-C. Indoor Air Quality Monitoring Systems for Enhanced Living Environments: A Review toward Sustainable Smart Cities. Sustainability 2020, 12, 4024. https://doi.org/10.3390/su12104024

[11] Xing Lu, Zhihong Pang, Yangyang Fu, Zheng O'Neill, The nexus of the indoor CO_2 concentration and ventilation demands underlying CO2-based demand-controlled ventilation in commercial buildings: A critical review, Building and Environment, Vol 218, 2022, 109116, ISSN 0360-1323, https://doi.org/10.1016/j.buildenv.2022.109116.

[12] Lee, Duk-Dong & Lee, Dae-Sik. (2001). Environmental Gas Sensors. Sensors Journal, IEEE. 1. 214 - 224. 10.1109/JSEN.2001.954834.

[13] Wetchakun, K & Samerjai, T & Tamaekong, Nittaya & Liewhiran, C & Siriwong, C & Kruefu, Viruntachar & Wisitsoraat, Anurat & Tuantranont, Adisorn & Phanichphant, Sukon. (2011). Semiconductor Metal Oxides as Sensors for Environmentally Hazardous Gases. Sensors and Actuators B Chemical. 160. 580-591. 10.1016/j.snb.2011.08.032.

[14] Chamberless NDIR CO_2 Sensor Robust against Environmental Fluctuations, Mostafa Vafaei and Amir Amini, ACS Sensors 2021 6 (4), 1536-1542 DOI: 10.1021/acssensors.0c01863

[15]Perez Rojas, Y.T. Measuring soil CO2 emissions with air-quality sensors. Nat Rev Earth Environ (2023). https://doi.org/10.1038/s43017-023-00435-8

[16] Hopper, R., Popa, D., Udrea, F. et al. Miniaturized thermal acoustic gas sensor based on a CMOS microhotplate and MEMS microphone. Sci Rep 12, 1690 (2022). https://doi.org/10.1038/s41598-022-05613-0
[17] Szafraniak, B.; Fu´snik, Ł.; Xu, J.; Gao, F.; Brudnik, A.; Rydosz, A. Semiconducting Metal Oxides: SrTiO3, BaTiO3 and BaSrTiO3 in Gas-Sensing Applications: A Review. Coatings 2021, 11, 185.doi.org/10.3390/coatings11020185
[18] Highly Selective CO2 Gas Sensing Properties of CaO-$BaTiO_3$ Heterostructures Effectuated through Discretely Created n-n Nanointerfaces, Shravanti Joshi, Frank Antolasic, Manorama V. Sunkara, Suresh K. Bhargava, and Samuel J. Ippolito, ACS Sustainable Chemistry & Engineering 2018 6 (3), 4086-4097, DOI:10.1021/acssuschemeng.7b04453
[19] C.N.R. Rao, "Perovskites", p707, Encyclopedia of Physical Science and Technology (Third Edition), 2003
[20] Johnsson, Mats, and Peter Lemmens. "Crystallography and chemistry of perovskites." arXiv preprint cond-mat/0506606 (2005)
[21] A.S. Bhalla, R. Guo and R. Roy, The perovskite structure – a review of its role in ceramic science and technology, Mat. Res. Innovat. 4, 3-26 (2000)
[22] ROOKSBY, H. Compounds of the Structural Type of Calcium Titanate. Nature 155, 484 (1945). https://doi.org/10.1038/155484a0
[23] Wainer E. and Salomon N. High titania dielectrics. Trans. Electrochem. Soc. 1946;89:331–56. doi: 10.1149/1.3071718.
[24] Ogawa T. On barium titanate ceramics. Busseiron Kenkyu. 1947;6:1–27.
[25] Vul B M. High and ultrahigh dielectric constant materials. Electrichestvo. 1946;3:12.
[26] Metal–organic framework based systems for CO_2 sensing, Andreea Gheorghe, Olivier Lugier , Bohui Ye and Stefania Tanase, DOI: 10.1039/D1TC02249K, J. Mater. Chem. C, 2021, 9, 16132-16142
[27] Goldschmidt, V.M. Die Gesetze der Krystallochemie. Naturwissenschaften 14, 477–485 (1926). https://doi.org/10.1007/BF01507527
[28]Global Barium Titanate Market, www.expertmarketresearch.com/reports/barium-titanate-market
[29] Ahmed M. El-Khawaga, Alaa Zidan, Ahmed I. A. Abd El-Mageed, Preparation methods of different nanomaterials for various potential applications: A review, Journal of Molecular Structure,Volume 1281,2023,135148,ISSN 0022-2860, https://doi.org/10.1016/j.molstruc.2023.135148.
[30] Sood, Ankur, et al. "A comprehensive review on barium titanate nanoparticles as a persuasive piezoelectric material for biomedical applications: prospects and challenges." Small 19.12 (2023): 2206401.
[31] Wong, Tak-Sing, Branden Brough, and Chih-Ming Ho. "Creation of functional micro/nano systems through top-down and bottom-up approaches." Molecular & cellular biomechanics: MCB 6.1 (2009): 1.
[32] Kubo, Teruichiro & Kato, Masanori & Fujita, Tadashi. (1967). Solid-Solid State Reactions between TiO2 and BaCO3. The Journal of the Society of Chemical Industry, Japan. 70. 847-853. 10.1246/nikkashi1898.70.6_847.
[33] Rezk, M.Y.; Sharma, J.; Gartia, M.R. Nanomaterial-Based CO_2 Sensors. Nanomaterials 2020, 10, 2251. https://doi.org/10.3390/nano10112251

[34] Almeida, G.N.; de Souza, R.N.; Lima, L.F.S.; Mohallem, N.D.S.; da Silva, E.P.; Silva, A.M.A. The Influence of the Synthesis Method on the Characteristics of BaTiO3. Materials 2023, 16, 3031. https://doi.org/10.3390/ma16083031
[35] Enhessari M, Salehabadi A. Perovskites-Based Nanomaterials for Chemical Sensors. Progresses in Chemical Sensor. InTech; 2016.http://dx.doi.org/10.5772/62559
[36] J. Mater. Chem. C, 2022,10, 10196-10223
[37] Perovskite-Based Gas Sensors,August 2022, DOI:10.1007/978-981-19-2685-3_12
[38] Bulemo, Peresi & Kim, Il-Doo. (2019). Recent advances in ABO3 perovskites: their gas-sensing performance as resistive-type gas sensors. Journal of the Korean Ceramic Society. 57. 10.1007/s43207-019-00003-1.
[39] J. Mater. Chem. C, 2022,10, 10196-10223
[40] Mahsa Souri, Hossein Salar Amoli, Gas sensing mechanisms in ABO_3 perovskite materials at room temperature: A review, Mat. Sc. in Semiconductor Processing, Vol.156,2023,107271,ISSN1369-8001, doi.org/10.1016/j.mssp.2022.107271
[41] Njegovec, M.; Donlagic, D. A Fiber-Optic Gas Sensor and Method for the Measurement of Refractive Index Dispersion in NIR. Sensors 2020, 20, 3717. https://doi.org/10.3390/s20133717
[42] Islam, S., Biswas, R.K. and Ghosh, J. (2019), Use of high temperature X-ray diffraction and pair distribution function for the study of carbonation characteristics of Barium Titanate at nanoscale. Micro Nano Lett., 14: 1204-1207